Reviews

Metal Hexacyanoferrates: Electrosynthesis, in Situ Characterization, and Applications

Norma R. de Tacconi* and Krishnan Rajeshwar

Department of Chemistry and Biochemistry, The University of Texas at Arlington, Arlington, Texas 76019-0065

Reynaldo O. Lezna

INIFTA, CONICET Universidad Nacional de La Plata, C.C. 16, Suc. 4, La Plata, (B1906ZAA), Argentina

Received March 13, 2003. Revised Manuscript Received June 5, 2003

This review focuses on the electrosynthesis, in situ characterization, and technological applications of Prussian blue analogues with the generic formula $A_hM_k[Fe(CN)_6]_l \cdot mH_2O$, where *h*, *k*, *l*, and *m* are stoichiometric numbers, A = alkali metal cation, and M is a transition metal. Six such metal hexacyanoferrate (MHCF) compounds derived from Cu, Pd, In, V, Co, and Ni are featured in this article against the backdrop of the Prussian blue parent compound itself and other related compounds. The use of cyclic voltammetry and complementary techniques including scanning probe microscopies, quartz crystal microgravimetry, and ac impedance spectroscopy, for studying the growth of MHCF films on targeted substrates, is discussed. Spectroelectrochemical in situ characterization of these films in the UV−visible and IR regions is then reviewed. Finally, the use of Prussian blue and its analogues in devices for displays and "smart" windows, photoimaging, environmental remediation, chemical/biological sensing, energy conversion, and magneto-optic/opto-magnetic switching is described. Electrocatalysis of targeted reactions and structural changes upon ion uptake by the MHCF compounds constitute the other topics in this review.

1. Introduction and Scope of Review

Transition metal hexacyanoferrates of the general formula $A_hM_k[Fe(CN)_6]_l \cdot mH_2O$ (*h*, *k*, *l*, *m* = stoichiometric numbers, A = alkali metal cation, M = transition metal ion) (Table 1) represent an important class of mixed-valence compounds, of which Prussian blue or iron(III) hexacyanoferrate(II) (with A = K and M = Fe in the above generic formula) is the classical prototype. Aside from their interesting solid-state chemistry and structural attributes, these compounds have garnered intense recent interest because of their electrocatalytic, electrochromic, ion-exchange, ion-sensing, and photomagnetic properties. While the electrochemistry and applications of Prussian blue itself have been rather extensively discussed,[1,2] only recently have the other transition metal analogues begun to receive attention.

In this review, we present a comparative discussion of the growth, in situ characterization, and applications of the Cu, Pd, In, V, Co, and Ni analogues. Our choice of these particular compounds for this review is simply motivated by the burgeoning literature on their applications, and by our own studies on them. After a primer on their solid-state chemistry, the growth of thin films of these compounds on targeted substrates is briefly discussed. In situ postdeposition characterization of these films, mainly by voltammetry, scanning probe microscopies, ac impedance spectroscopy, and spectroelectrochemical methods, is then reviewed. Finally, recent studies focusing on practical applications of these materials are discussed. The references cited in each instance are representative rather than comprehensive.

The chemistry of mixed-valence compounds has been extensively discussed by previous authors.[1−6] The structural aspects and electrochemistry of Prussian blue itself have been previously reviewed.[7,8] Many of the compounds addressed in the present review have been described in terms of their electrochromic properties.[2] Finally, the magnetic properties of Prussian blue analogues have also been discussed.[9] Every attempt has been made to avoid redundancy between these earlier treatments and the present review, while unavoidable areas of overlap will be highlighted in what follows.

2. Solid-State Chemistry and Electrochemistry of Metal Hexacyanoferrates

Metal hexacyanoferrates have a face-centered cubic lattice (unit cell length: ∼10.2 Å) with octahedral co-

* To whom correspondence should be addressed. E-mail: ntacconi@uta.edu.

10.1021/cm0341540 CCC: $25.00
Published on Web 07/08/2003

Table 1. Compound Stoichiometries and Metal Oxidation States in Prussian Blue (MHCF) Analogues

metal	formula	M:Fe ratio	M, Fe formal oxidation state[a]
copper	$K_2Cu_3[Fe(CN)_6]_2$	3:2	II, II
	$Cu_3[Fe(CN)_6]_2$	3:2	II, III
palladium	$K_2Pd_3[Fe(CN)_6]_2$	3:2	II, II
	$Pd_3[Fe(CN)_6]_2$	3:2	II, III
	$K_2Pd[Fe(CN)_6]$	1:1	II, II
	$KPd[Fe(CN)_6]$	1:1	II, III
indium	$In_4[Fe(CN)_6]_3$	4:3	III, II
	$KIn_4[Fe(CN)_6]_3(SO_4)_2$	4:3	III, III
	$KIn[Fe(CN)_6]$	1:1	III, II
	$In[Fe(CN)_6]$	1:1	III, III
vanadium	$K_2(VO)_3[Fe(CN)_6]_2$	3:2	II, II
	$(VO)_3[Fe(CN)_6]_2$	3:2	II, III
	$K_3(VO_2)_3[Fe(CN)_6]_2$	3:2	I, III
	$K_{1.4}(VO)_{1.3}[Fe(CN)_6]$	4:3	II, II
	$K_{0.4}(VO)_{1.3}[Fe(CN)_6]$	4:3	II, III
cobalt	$K_2Co_3[Fe(CN)_6]_2$	3:2	II, II
	$Co_3[Fe(CN)_6]_2$	3:2	II, III
	$K_{1.4}Co_{1.3}[Fe(CN)_6]$	4:3	II, II
	$K_{0.4}Co_{1.3}[Fe(CN)_6]$	4:3	II, III
	$K_2Co[Fe(CN)_6]$	1:1	II, II
	$KCo[Fe(CN)_6]$	1:1	II, III
	$Co[Fe(CN)_6]$	1:1	III, III
nickel	$K_2Ni_3[Fe(CN)_6]_2$	3:2	II, II
	$Ni_3[Fe(CN)_6]_2$	3:2	II, III
	$K_2Ni[Fe(CN)_6]$	1:1	II, II
	$KNi[Fe(CN)_6]$	1:1	II, III

[a] The oxidation state, in the case of vanadium, refers to oxygen-bonded species rather than the "free" metal cation; see text.

ordination of the M and Fe ions by −N≡C and −C≡N ligands, respectively.[10,11] The alkali metal cations, A (which provide charge compensation), are located in the tetrahedral sites[12] in these structures, which may also contain coordinated water molecules and anions in some cases. Representative structures and the corresponding compound stoichiometries are contained in Figure 1 for M and Fe in the +2 and +3 oxidation states, respectively. Table 1 provides a listing of the electrochemically relevant compounds along with the corresponding M:Fe stoichiometries and formal oxidation states of the M and Fe sites for the six metals considered in this review.

A change on the M oxidation state from +2 to +3 brings about a contraction of the M octahedral coordination manifold. This in turn manifiests as a decrease in the unit cell dimension—a trend particularly well-exemplified by the CoHCF compound system. In contrast, the octahedral coordination geometry is not significantly perturbed in size by the Fe oxidation state, as borne out by the similarity between the unit cell parameters of $K_4[Fe(CN)_6]$ and $K_3[Fe(CN)_6]$, respectively.[4]

In the case of the vanadium analogue, X-ray photoelectron spectroscopy (XPS) and IR evidence[13,14] support the presence of VO^{2+} (vanadyl) ions in the compound structure. This would imply an octahedral coordination environment for the vanadium metal sites in which one of the six bridging CN ligands is occupied by a terminal oxygen. On the other hand, the measured V:Fe ratio of 1.5 ± 0.03[14] suggests a trend in the vanadium system that is common with the Cu, Pd, In, Co, and Ni analogues (Figure 1 and Table 1). Contrasting with an earlier study,[13] evidence has been presented[14] for redox

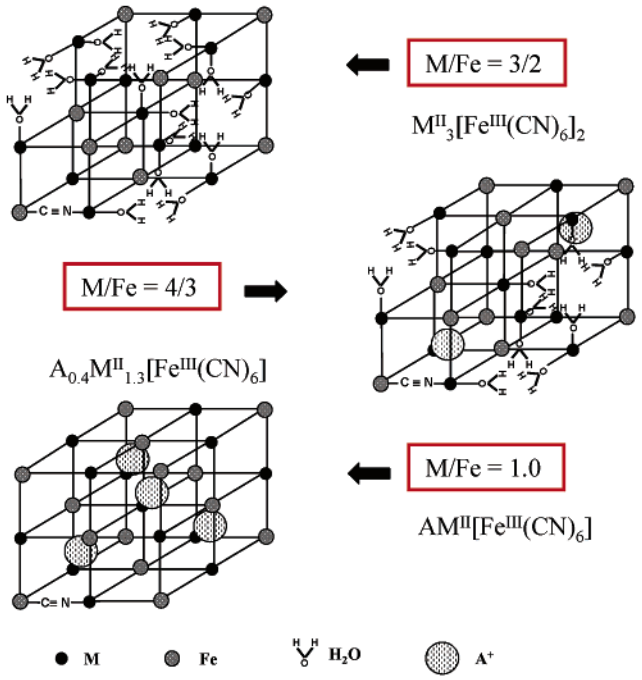

Figure 1. Unit cell representation of $M_3[Fe(CN)_6]_2$, $A_{0.4}M_{1.3}[Fe(CN)_6]$, and $AM[Fe(CN)_6]$. The A^+ cations are located in the cell interstitial sites, and the cyanide groups are between M and Fe but have been largely omitted in this representation for the sake of clarity.

transitions in this compound to involve only the Fe sites, leaving the VO^{2+} sites intact. There are exceptions to this trend as noted later in this review. The simplified notation, VHCF, is used below with the implication that the vanadium metal cation is not present in the "free" state.

Mixed metal hexacyanoferrates have been prepared both as thin films and bulk precipitates (powders), as exemplified by the following compound: $K_{1.74-2y}Pd_y^{II}Ni_{1.13}^{II}[Fe^{II}(CN)_6]$ (where $y < 0.72$).[15] Rather than simple incorporation of Pd^{2+} at interstitial lattice positions, it has been hypothesized that, at higher Pd^{2+} levels in solutions, palladium ions occupy nominally Ni positions in a −N≡C coordinated environment.[15] Similar Ni/Co hybrid hexacyanoferrate networks have also been described.[16]

By tuning the oxidation state of the iron sites, it has been shown that the Ni or the In analogues behave either as redox-conducting solid electrolytes or as semiconductor/insulator materials.[17] Thus, the fully oxidized or fully reduced form of the Ni analogue shows the voltammetric profile of an insulator. On the other hand, the mixed-valence form containing both Fe^{II} and Fe^{III} redox sites shows semiconductor behavior. These data underline the fact that the interplay between electron and ion fluxes depends on the openness of the structural network to ion motion and to factors such as hydration. Indeed, electron diffusion in wet and dry Prussian blue films has been interrogated on interdigitated array electrodes.[18] Other evidence from dc conductivity measurements shows a predominantly site-wise electron-hopping mechanism in truly dry Prussian blue and substituted metal analogues.[19] Uptake of water provokes ionic conductivity in the system, and to the extent that electron hopping is coupled with ion motion to preserve local charge neutrality, hydration of the

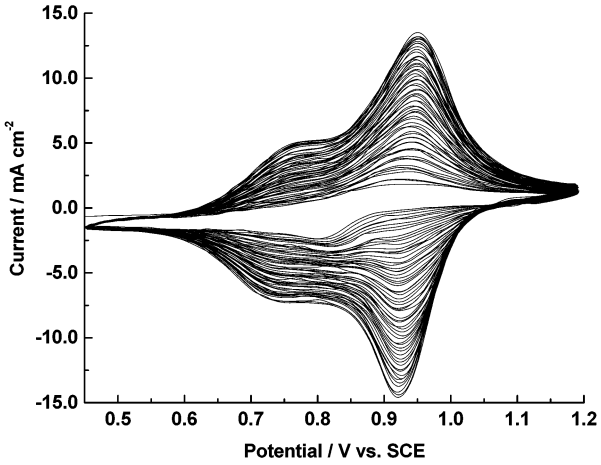

Figure 2. Cyclic voltammograms recorded during the growth of VHCF films on platinum substrates. The electrolytic solution consisted of 1×10^{-3} M $K_3[Fe(CN)_6] + 1 \times 10^{-3}$ M $NaVO_3$ in 3.6 M $H_2SO_4 + 0.2$ M K_2SO_4. The platinum electrode was kept polarized at 1.2 V in 3.6 M $H_2SO_4 + 0.2$ M K_2SO_4 during the addition of the film precursor species to avoid incipient chemical coagulation of VHCF on the electrode surface. 50 potentiodynamic growth cycles at 100 mV s^{-1}.

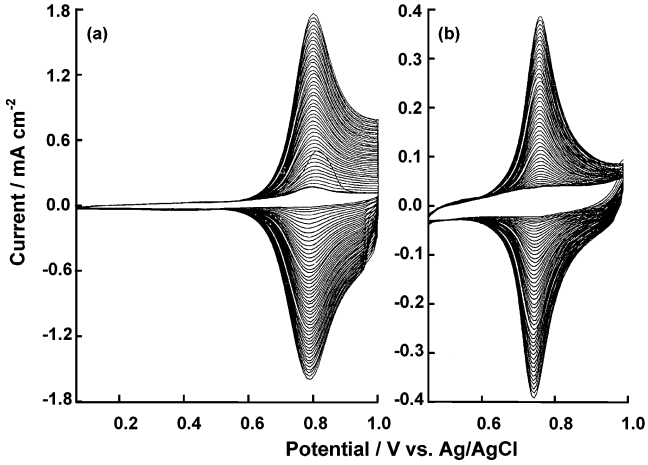

Figure 3. Cyclic voltammograms recorded during the growth of an InHCF film on a gold substrate using an extended (a) and a restricted potential window (b). Solution composition: 5×10^{-4} M $K_3[Fe(CN)_6]$ and 2.5×10^{-4} M $In_2(SO_4)_3$ in 0.5 M K_2SO_4 of pH 2. 50 potentiodynamic growth cycles at 50 mV s^{-1}.

material becomes an important factor in its overall charge transport behavior.[17,20]

Other aspects of the solid-state chemistry of metal hexacyanoferrates (including that of the parent, Prussian blue) have been discussed by previous authors.[1−8,10,11, 21]

3. Electrosynthesis

Prussian blue itself has been prepared by both chemical[22,23] and electrochemical[24,25] methods. Here, we will confine our discussion mostly to supported films of the metal hexacyanoferrate (MHCF) compounds. The most common strategy for electrosynthesis involves potentiodynamic cycling between pre-set potential limits of the working electrode in a supporting electrolyte containing both the metal ion (M^{n+}) and ferricyanide species. The metal ion can be dosed in situ into the growth medium from an active metal anode. This method has been used for the growth of the copper[26] and nickel[27−29] analogues. In other instances inert substrates such as glassy carbon, graphite, platinum, or gold are used. In these cases, the metal ions are added to the ferricyanide-loaded supporting electrolyte. Potentiodynamic cycling then instigates in situ precipitation of the (insoluble) MHCF compound on the inert film substrate surface. For applications wherein optical transparency of the entire film assembly is desired, conducting transparent oxide supports such as tin-doped indium oxide or F-doped SnO_2 glass may be used.

Figure 2 contains representative cyclic voltammograms, signaling the growth of a VHCF film on a Pt substrate. Other than voltammetry, electrochemical quartz crystal microgravimetry (EQCM)[30,31] affords a sensitive probe of the mechanistic details associated with MHCF film growth. Such measurements have been described, for example, for InHCF[32] and NiHCF[33] during film growth. Elemental analysis via atomic spectroscopy and XPS provides confirmation of the identity of the specific compound that has been deposited. The M:Fe atom ratio is a useful parameter in this regard (Table 1), as has been shown, for example, for the In,[34] V,[14] Co,[35] and Ni[36] analogues. Mössbauer studies have been reported[37] for CoHCF wherein the $Fe^{II/III}$ mixed-valent state was induced by ozonation. A very broad new line for the mixed-valent state was detected.[37]

The stoichiometric composition of the MHCF films prepared by electrosynthesis depends not only on the potential window but also on the number of potentiodynamic growth cycles used. This is well-exemplified by the InHCF system.[32,38] Broader growth cyclic voltammetry profiles were discerned under "extended potential window" (EPW) conditions relative to the "restricted potential window" (RPW) case.[38] This is shown in Figure 3. The EPW film also grew at a faster rate compared to its RPW counterpart; compare the ordinate current scales in the two cases in Figure 3. These differences were rationalized on the basis that, apart from the 1:1 (In:Fe) compound stoichiometry (Table 1), the 4:3 compound is also formed under the EPW condition.[38] In the CoHCF system, XPS data show the Co:Fe ratio in the film to increase with the film thickness, that is, with increasing number of growth cycles.[35]

Another striking example of the sensitivity of film morphology to the growth history is provided by the cyclic voltammetry and atomic force microscopy data in Figures 4 and 5, respectively, for the CoHCF system.[35] The three cases shown differ in the adjustment of the initial coagulation period prior to the electrosynthesis step and the extent of passivation of the gold substrate. Note that in the last case (Figures 4c and 5c) there is virtually no in situ precipitation when the potentiodynamic growth cycle is initiated. With a 20-min coagulation period (Figures 4b and 5b), the voltammetry profile is diagnostic of substantial CoHCF formation already when the potentiodynamic growth cycle is initiated (Figure 4b). The film morphology is roughest in this case (Figure 5b). The corresponding ac impedance spectroscopy (ACIS) data of the CoHCF films in the three instances also exhibit interesting differences.[39] For example, Figure 6 compares the ACIS profiles for a thin and a thick CoHCF film. The model simulations (shown

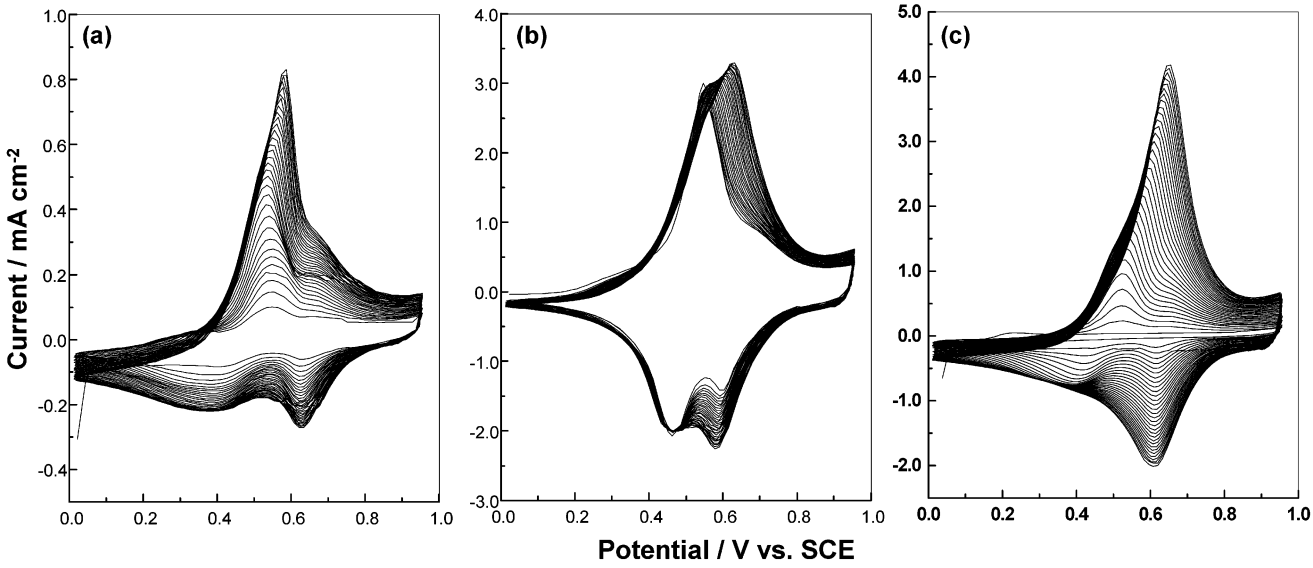

Figure 4. Cyclic voltammograms recorded during the growth of CoHCF films on gold substrates using 1×10^{-3} M $K_3[Fe(CN)_6]$ + 1×10^{-3} M $Co(NO_3)_2$ mixed in deoxygenated 1 M KNO_3. 30 potentiodynamic growth cycles at 50 mV s^{-1}. (a) Electrochemical thin film ($\delta = 80$ nm) on nonprotected gold, (b) chemical thick film ($\delta = 320$ nm) (20 min at open circuit in precursor solution), and (c) electrochemical thick film ($\delta = 335$ nm) on electrochemically protected gold.

as asterisk marks in the fits to experimental data in Figure 6; these are described in detail in ref 39) indicate a larger number of resistance and capacitance (RC) relaxations in the thicker film—a trend that is in good agreement with the cyclic voltammetry and spectroelectrochemical data.

A method that is potentially applicable to the preparation of multilayers of MHCFs with different metal analogues has been described.[40] Self-assembly of mercaptopropionic acid was followed by subsequent attachment of CuHCF to the thiol and carboxylate functionalities of the template layer.[40] Multiple sequential adsorption of metal ions and hexacyanometalate anions was also used to deposit several MHCF analogues on solid supports with monolayer precision.[41,42] Other studies oriented toward the preparation of Langmuir–Blodgett films of Prussian blue are exemplified by ref 43. Highly ordered Prussian blue nanowire arrays (nanowire diameter: ~50 nm; length: up to 4 μm) were fabricated[44] using electrodeposition in an alumina (alumite) template.[45] Finally, CuHCF (and other magnetic compounds) were prepared on the nanometer-size scale by controlled coprecipitation involving mixtures of water-in-oil microemulsions.[46]

Metal hexacyanoferrate compounds can also be mated with semiconductor particles.[47] In the electrosynthetic approach, the growth medium is simply dosed with the semiconductor particles to the desired level (usually in the range of several mg/L). Alternately, a single-crystal semiconductor surface can be coated with MHCF via electrodeposition, as demonstrated for n-TiO_2[48] and n-$SrTiO_3$.[49] A variant of this approach involves the use of polycrystalline semiconductor films on which the MHCF layer is subsequently coated.[50–52] Finally, metal/semiconductor (M/S) composite coatings can be subsequently derivatized by exposing them to ferricyanide.[53–55] The M component in the composite is converted in situ to the corresponding MHCF layer (see above) in this manner. The example contained in Figure 7 for the InHCF case illustrates that (a) the morphology of the TiO_2 film is sensitive to the presence of In islands in the composite and (b) the presence of In has a "catalytic" influence on InHCF film growth (cf., the growth profiles in Figures 3a and 7b).

Applications of the above composites in electrochromic, photochromic, and photocatalytic applications will be discussed later in this review. The reader is also referred to other studies[13,14,56–61] for further details of MHCF film growth by electrochemical methods.

4. Redox Transformations and Ion Fluxes

Once the MHCF layer is grown on a targeted surface, the chemically modified electrode assembly can be transferred to a medium containing only the supporting electrolyte. Subsequent cyclic voltammetry reveals one or more reversible waves, signaling redox processes of the MHCF layer. The complexity of this voltammogram depends on the particular system, and how many compound stoichiometries (Table 1) are inherent in the deposited layer, but particularly clean profiles are seen for the Cu and In analogues (the latter under a restricted potential window growth condition, see above) as shown in (a) and (b), respectively, of Figure 8. Note that the voltammetry waves in this figure are sharp and symmetrical and have no diffusion tail in either positive- or negative-going cycles. Further, the peak potential separation is close to zero in both the cases. These trends are diagnostic of the surface-confined location of the MHCF redox process.[62,63]

Pertinent here is the influence of counterion motion on the voltammogram profiles. Recall that alkali cation flux in to and out of the MHCF layer is critical to maintaining local charge neutrality during film redox.[63] Even early studies[64,65] on this topic revealed the sensitivity of the voltammetry profiles to electrolyte cations. For example, the introduction of Cs^+ caused multiple wave formation in the NiHCF system; interestingly, changing the supporting cation from one to another and then back to the first reproduced the original cyclic voltammo-

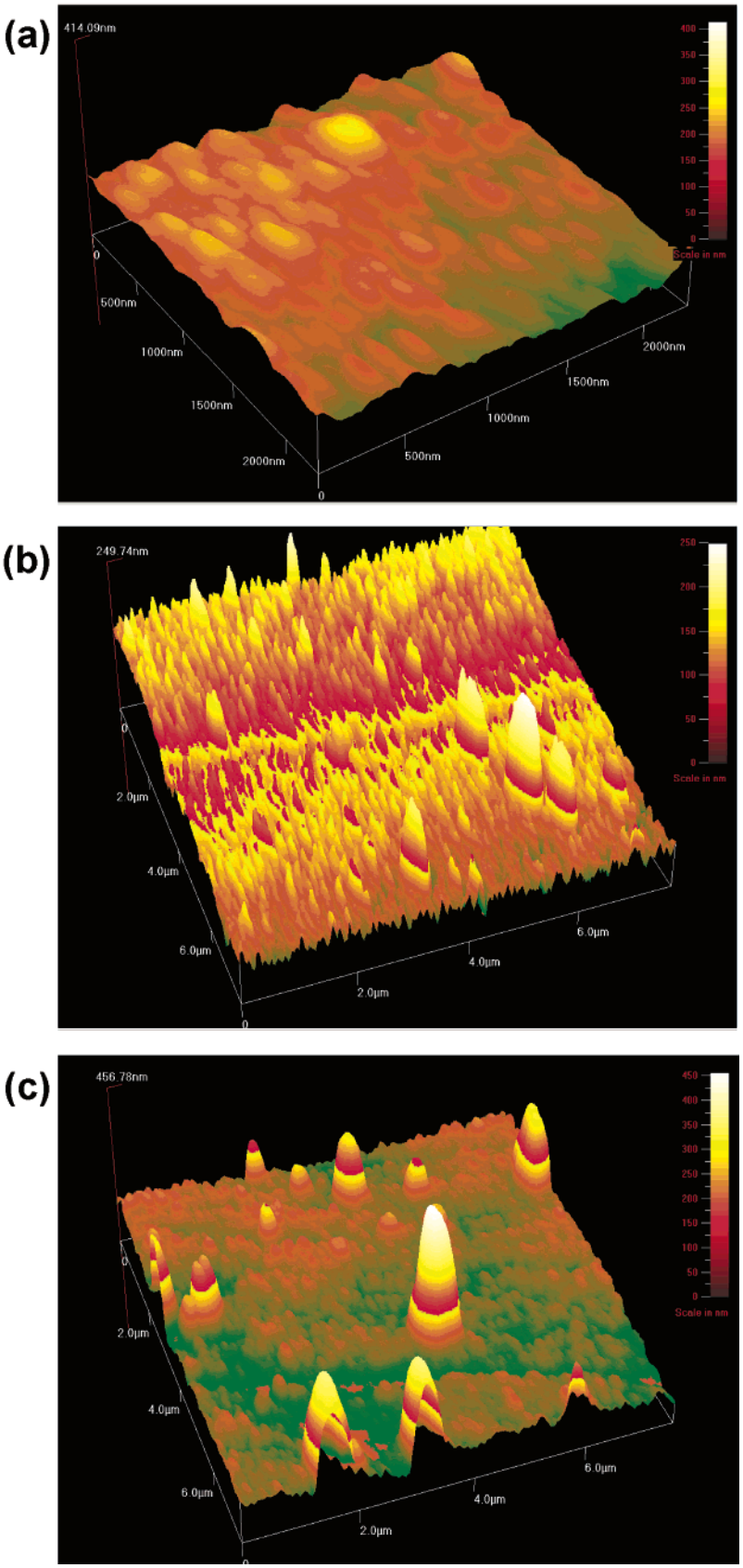

Figure 5. Atomic force microscopy images (taken in noncontact mode) of three CoHCF films on gold that were prepared according to details provided in the caption in Figure 4.

gram.[64] The redox reaction in CuHCF was seen to be faster in an ammonium-ion-containing medium than in K^+-containing electrolytes.[65] Nernstian semilog plots of peak potentials versus the ammonium ion concentration were also presented in this early study.[65] Similar data exist for K^+, NH_4^+, or Na^+ ions in the CuHCF and CoHCF systems.[66−68] The analytical implications of these data are deferred to a subsequent section.

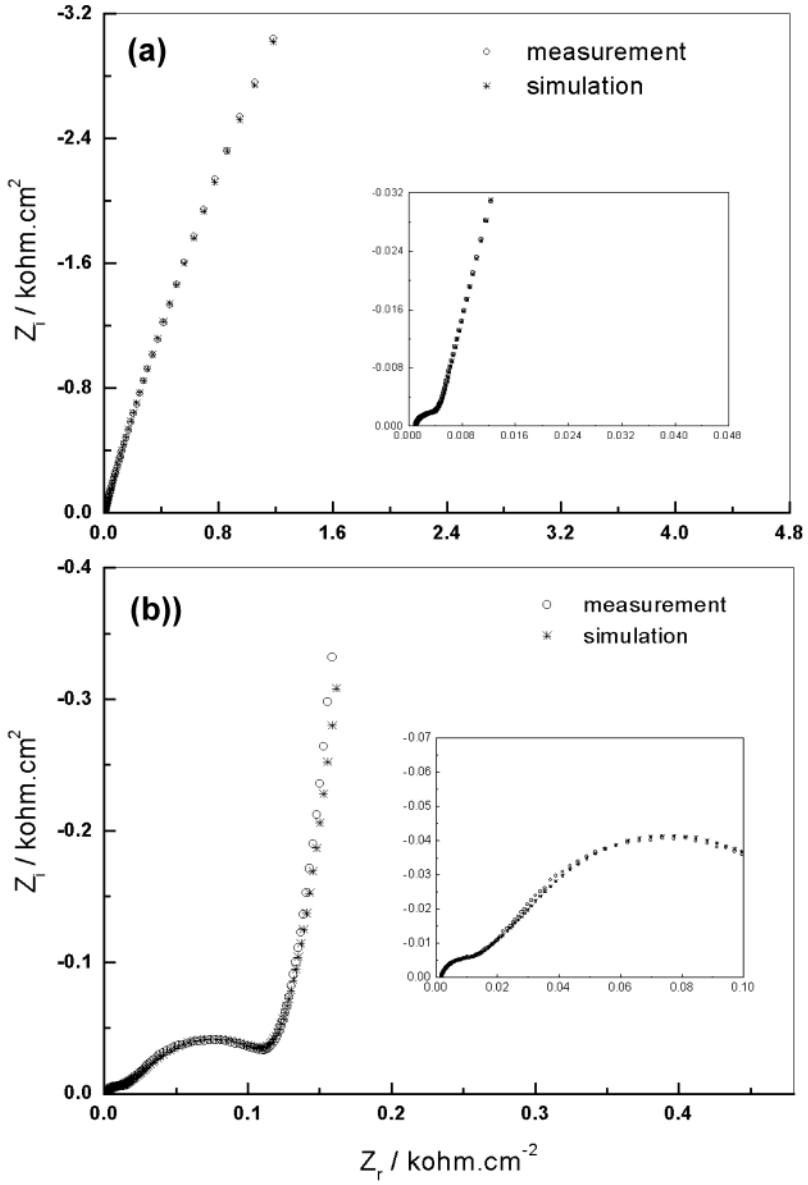

Figure 6. ac impedance spectroscopy data presented in the form of Nyquist plots for a thin (Figure 6a) and thick (Figure 6b) CoHCF film in deoxygenated 1 M KNO_3 electrolyte. Both the experimental data (○) and the model fits (*) are shown. Details of the simulations are contained in ref 39. The inserts show the high-frequency portion of the data in enlarged fashion. All spectra are acquired at open-circuit.

Loss of electroactivity has been observed for Rb^+- and Cs^+-containing electrolytes when CoHCF films are voltammetrically cycled.[61,69] These changes in electroactivity were attributed to the rather large hydrated radii of Rb^+ and Cs^+ ions and inhibition of their ingress/egress in to/out of the MHCF framework. Similar voltammetric "passivation" of the CoHCF film in Li^+-containing electrolytes has been attributed to the large hydration sphere of Li^+ cations.[61] The formal potentials of CoHCF films were measured for Li^+-, Na^+-, K^+-, and Cs^+-containing electrolytes and were found to correlate well with the sizes of the hydrated ions.[70] Ion permeability in an InHCF film was reported to follow the order $Na^+ > K^+ > NH_4^+ > Li^+$ in two separate studies.[71,72] Cyclic voltammograms were presented for NiHCF films in 13 different cation-containing supporting electrolytes.[60] Other voltammetric studies pertaining to the effect of electrolyte cations include ref 73 on CoHCF. Once again, the ACIS technique provides a sensitive probe of the counterion fluxes in MHCF. Figure 9 contains a comparison of the ACIS profiles for CoHCF in Na^+-, K^+-, and Rb^+-containing electrolytes. Exchange current densities can be extracted from model simulations of these data[39] and are 15.2, 6.9, and 0.12 mA cm^{-2} for the three counterions, respectively. Clearly, the hydrated radii play a critical role in the ease of transport of these ions in/out of the MHCF framework.

The EQCM probe affords another sensitive in situ probe of the ion fluxes during MHCF film redox. This is exemplified by measurements on InHCF,[68] CoHCF,[60,70] and NiHCF.[60,74] The probe beam deflection technique was employed for monitoring ion transport during redox of InHCF surface layers.[75] The principal charge-compensating ions were shown[75] to be cations (but see below). X-ray absorption near-edge structure (XANES) experiments indicate that the chemical environment of Co(II) sites are influenced by the presence of hydrated alkali metal counterions.[70] Finally, oxida-

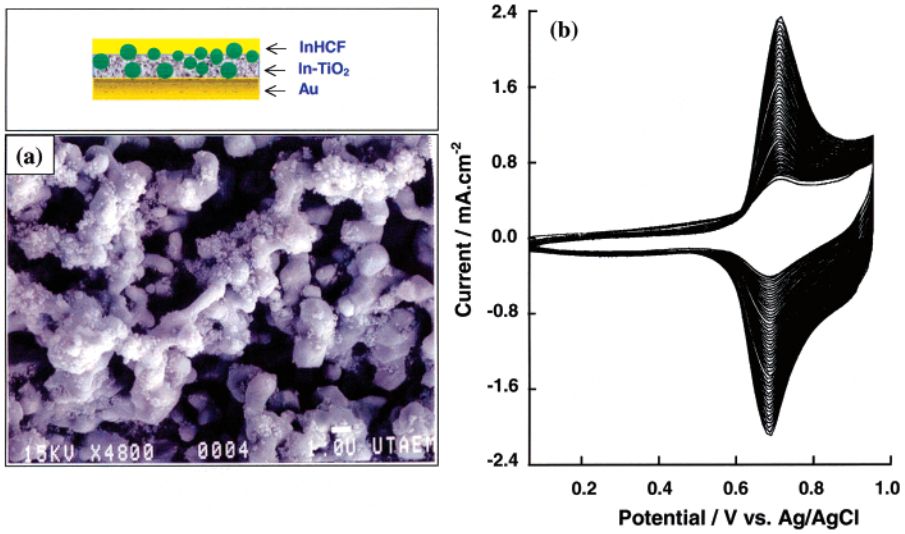

Figure 7. SEM micrograph of an In−TiO_2 composite film grown on a gold substrate (Figure 7a) and the corresponding growth of a top layer of InHCF by repetitive cycling in a solution containing 5×10^{-4} M $K_3[Fe(CN)_6]$ and 2.5×10^{-4} M $In_2(SO_4)_3$ in 0.5 M K_2SO_4 (pH 4.5) (Figure 7b). 30 potentiodynamic growth cycles at 50 mV s^{-1}. A schematic illustration of the In−TiO_2 composite film derivatized with InHCF is shown in the top left side of this figure.

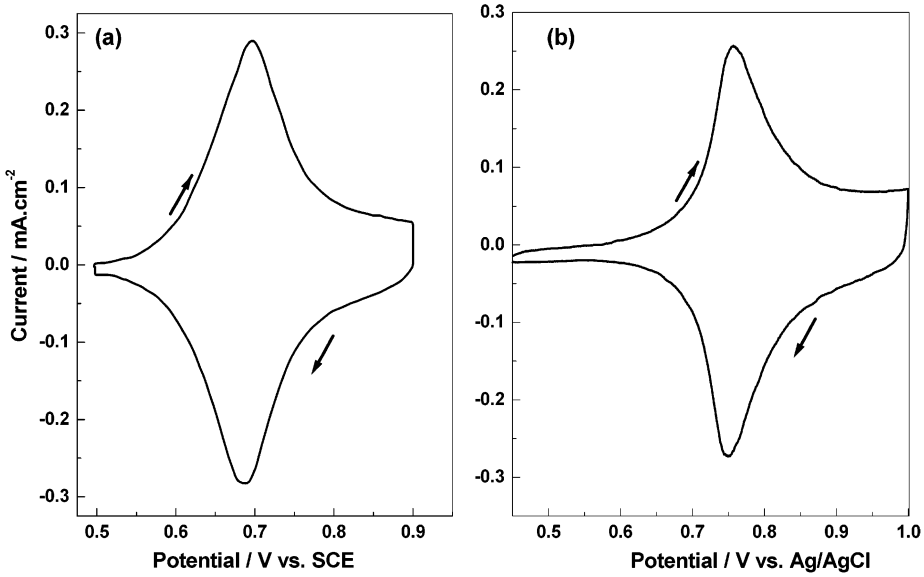

Figure 8. Cyclic voltammograms for a CuHCF film in contact with 0.5 M K_2SO_4 at a scan rate of 3.2 mV s^{-1} (Figure 8a) and a InHCF film in 0.5 M K_2SO_4 (pH 2) at 5 mV s^{-1} (Figure 8b).

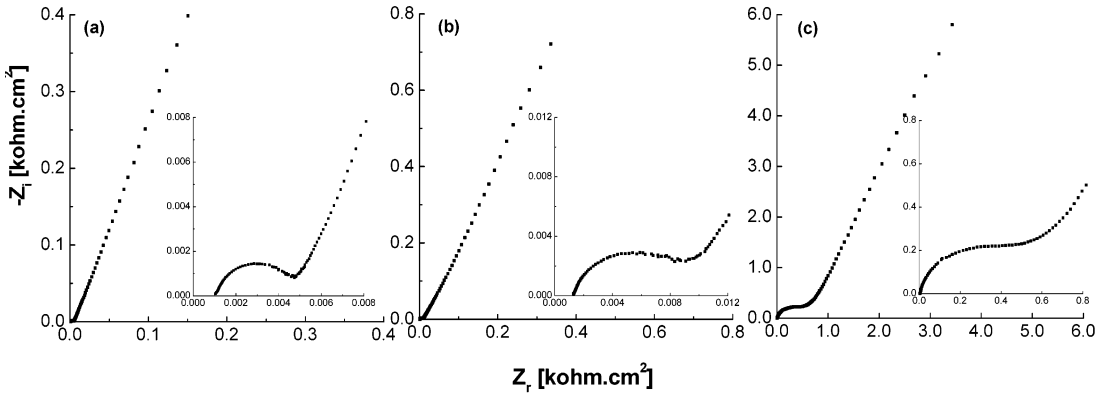

Figure 9. ac impedance spectroscopy profiles for CoHCF in contact with Na^+, K^+, and Rb^+ ion-containing electrolytes. All ions are at 0.1 M. Other experimental conditions and details as in Figure 7.

tion state profiles in NiHCF-derivatized electrodes were mapped with the use of line-imaging Raman spectroscopy.[76]

While alkali cations are the principal charge-compensating species during redox of MHCF films, radiotracer evidence on InHCF points toward contributions from

Scheme 1

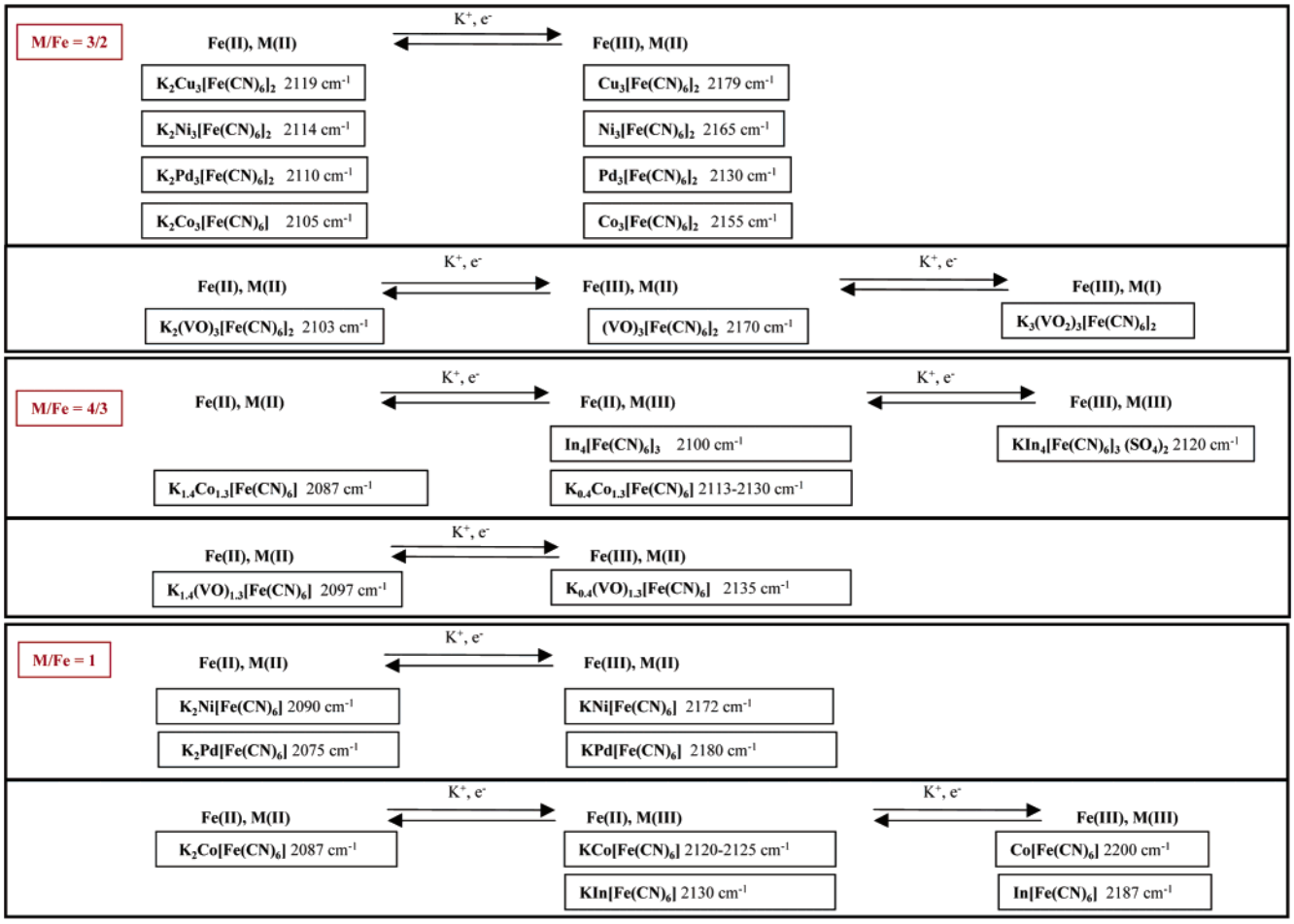

M = Cu, Ni, Pd, In, Co, VO, VO_2

anion fluxes as well.[68] This manifests mainly for the M:Fe 4:3 compound stoichiometry (see also Table 1). Anion fluxes are also shown both by survey XPS scans and quantitative assays for S (arising from sulfate anions) in the InHCF system.[38] Similar behavior appears to hold in the vanadium case.[14] Interestingly, the probe beam deflection technique indicated a contribution to anion fluxes in InHCF of only <7%, at least for film potentials below 0.9 V (versus saturated calomel electrode reference).[75] The double injection of electrons and cations was also studied by monitoring time-resolved changes in the optical reflectivity of Prussian blue-modified Pt disk electrodes during galvanostatic reduction of the film.[77]

Scheme 1 provides a compilation of the redox transformations and the corresponding compound compositions for the various members of the MHCF family. This scheme was synthesized from the cyclic voltammetry, ACIS, and spectroelectrochemical behavior of the various MHCF compounds. The ion-exchanger application that is suggested by the above discussion for these compounds is deferred to a subsequent section of this review. The issue of ion uptake and changes in the MHCF compound architecture will be further discussed in that section.

5. Spectroelectrochemistry

Spectroelectrochemistry combines two powerful techniques, namely, spectroscopy and electrochemistry, for studying the changes occurring during redox of the test system.[78−82] Thus, oxidation states can be changed electrochemically by addition or removal of electrons at an electrode while spectral measurements on the electrode surface or on the solution adjacent to the electrode or within a thin-layer cell are made simultaneously. Importantly, this combined approach obviates a key shortcoming of electrochemical probes associated with their chemical nonspecificity.[83] In this section, the application of IR and UV−visible spectroelectrochemical probes to the MHCF system will be reviewed.

Infrared and Raman spectroscopies are sensitive and versatile probes of the cyanide group stretching vibration region (ca. 2000−2250 cm^{-1}) in the MHCF family.[21,29,84−87] The corresponding IR signatures for the various compounds of interest here are listed in Scheme 1. Ex situ diffuse reflectance Fourier transform (FT) IR data were presented for NiHCF in an early study,[29] and the virtues associated with acquiring the spectra in situ in an electrochemical cell (i.e., in a spectroelectrochemical experiment) were pointed out by these authors. We will now present more recent examples drawn from our own studies on the MHCF compounds.

The following data in Figure 10 were obtained in the reflectance mode and the output was examined as the normalized difference between the signal at a given potential and that from the electrode without the MHCF film taken as reference, R_{ref}, that is, $R/R_{ref} = (R - R_{ref})/R_{ref}$. The changes in the spectral bands as the applied

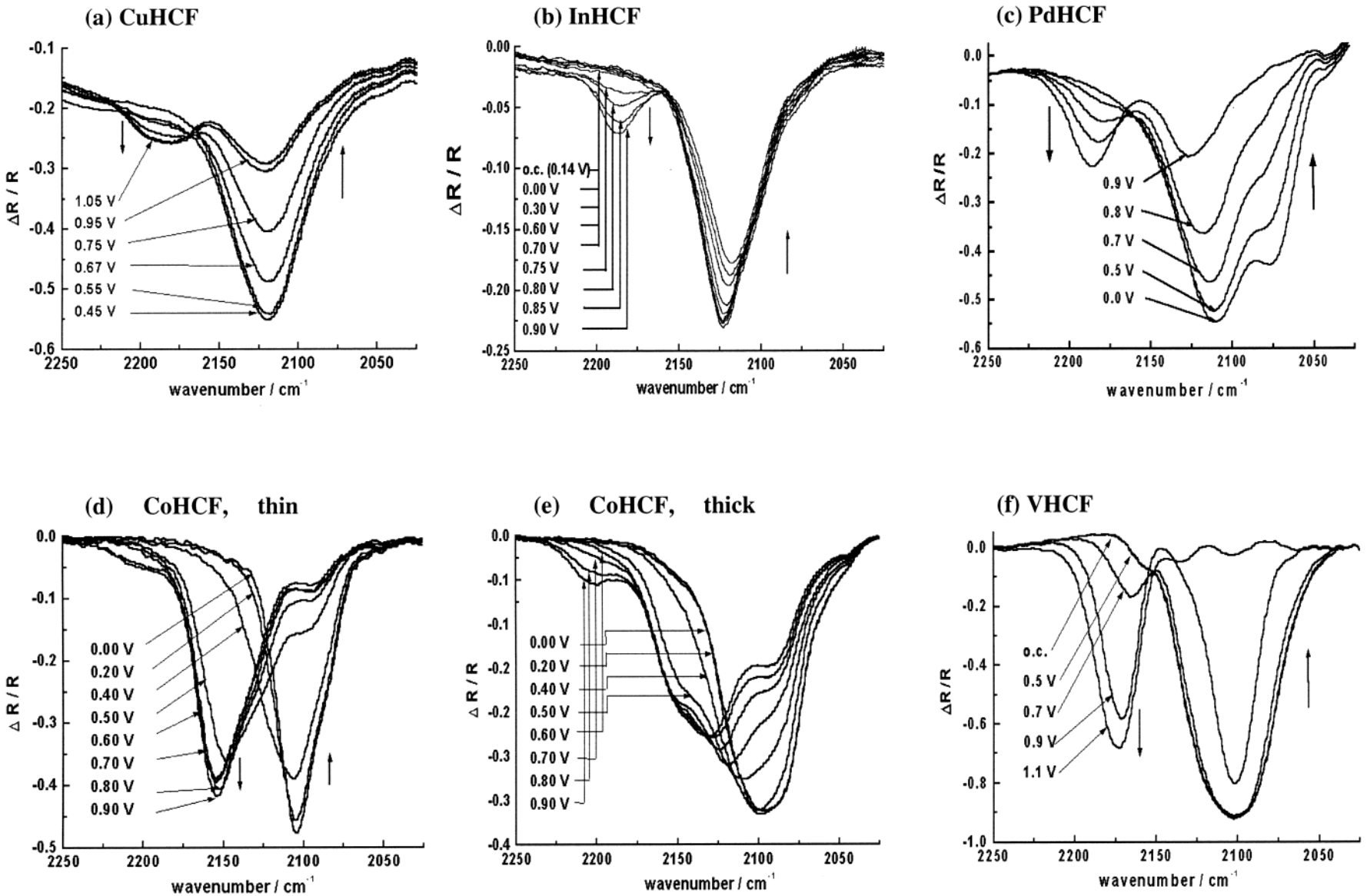

Figure 10. In situ infrared reflectance spectra of five MHCF compounds. All spectra were obtained at stepwise increasing potentials that are indicated in each set of spectra. (a) CuHCF in 0.5 M K_2SO_4, (b) InHCF in 0.5 M K_2SO_4 (pH 2) and for EPW conditions, (c) PdHCF in 1 M KCl (pH 2.5), (d and e) CoHCF thin (surface loading, $\Gamma = 6 \times 10^{-8}$ mol/cm^2) and thick film ($\Gamma = 2 \times 10^{-7}$ mol/cm^2), respectively, and in M KNO_3, and (f) VHCF in 3.6 M H_2SO_4 + 0.2 M K_2SO_4.

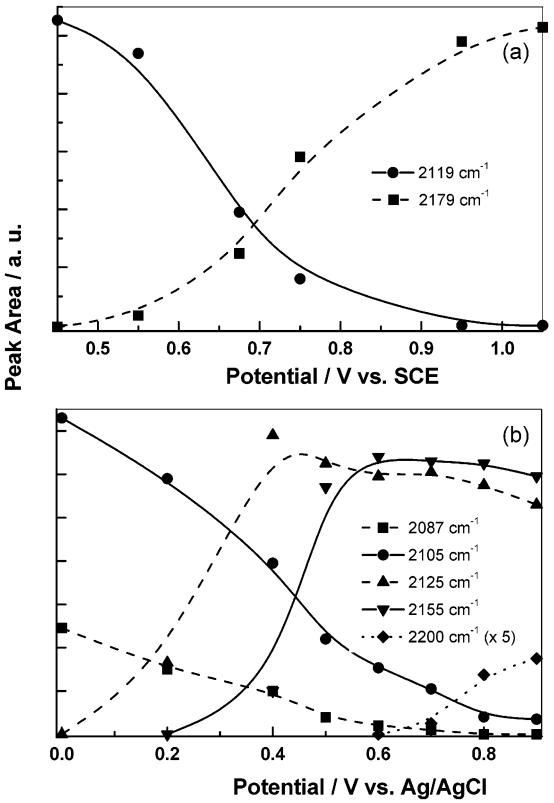

Figure 11. Peak areas of deconvoluted infrared bands as a function of potential for CuHCF (Figure 11a) and CoHCF (Figure 11b) films. The areas were obtained from the spectra shown in (a) and (d), respectively, of Figure 10.

potential is sequentially changed report on the redox conversion of the particular MHCF studied. Further, the complexity of the acquired in situ spectral profiles points toward the possibility of multiple compound formation in each system (see Table 1 and Scheme 1). Thus, the profiles are particularly simple for CuHCF (Figure 10a) and InHCF (Figure 10b). The complexity then follows the order PdHCF < CoHCF < VHCF.

Sample in situ IR spectroelectrochemical data for these compounds are shown in Figure 10 for five analogues. The behavior of PdHCF[88] and CoHCF[35] has been amplified elsewhere; that of VHCF is particularly complex (Figure 10f) and at least four participant species appear to be implicated in the redox process (see Scheme 1). The redox transformations undergone by the various participating species in each system (Table 1) can be better discerned by plotting the peak area of the deconvoluted IR bands as a function of potential. Two examples of such plots are shown for CuHCF (Figure 11a)[89] and CoHCF (Figure 11b),[35] respectively. The differences in the complexity of the overall redox process are striking in the two cases considered. Finally, it must be pointed out that the spectral changes shown in Figures 10 and 11 as a function of potential are completely reversible in that comparable data are obtained by stepping the potential back in the opposite direction.

Turning to spectroelectrochemistry, with the spectral changes monitored in the UV−visible region, the data can be acquired in situ either in the transmission mode or in the reflectance mode. In an early study,[90] diffuse reflectance UV−visible spectroelectrochemistry on Ni-HCF was shown to be both species-specific and sensitive to the amount of surface-confined material (on the electrode surface) and its oxidation state. Another useful approach involves acquisition of the UV−visible spectral data (at selected wavelengths) while the electrode potential is slowly scanned as in a voltammetry experiment.[63,88,91] The resultant data, processed in the form of the time derivative signal versus electrode potential, bear a striking resemblance to cyclic voltammograms but with the important distinction that the scans are *species-specific*.[63,88,91] Such data have been presented for CoHCF.[92] UV−visible spectroelectrochemistry has also been utilized to determine the electron stoichiometry during redox of InHCF in aqueous electrolytes,[71] according to methodology developed by other authors.[93]

Table 2. Wavelength Maxima for the Oxidized and Reduced Redox States of MHCF Compounds

	λ_{max}, nm (ϵ, M^{-1} cm^{-1})[a]	
compound	oxidized state(s)	reduced state(s)
CuHCF	405	495 (1900)
InHCF	495 (1660)	360
PdHCF	440	425 (940)
CoHCF	440 (580), 530 (1950)	380
NiHCF[b]	405	320
VHCF	515, 600, 780	390 (2250), 455 (760)

[a] Values of the molar extinction coefficients (ϵ) were calculated from the expression: $\ln[1 + (\Delta R/R)] = [-2.1000\epsilon/(nFS \cos \phi)]\Delta Q$ as elaborated in ref 89. [b] From ref 90.

Our own UV−visible spectroelectrochemical studies on the MHCF system were performed on a custom-built optical multichannel analyzer fitted with a cooled Si diode array detector.[88,94−96] Reflectance spectra were acquired during slow (nominally 5 mV s^{-1}) voltammetric scans of the MHCF-modified gold electrodes. The data (see below) are displayed as plots of $\Delta R/R$ versus the wavelength. Unlike in the IR cases discussed earlier, the ordinate values in the UV−visible experiments are normalized to a reference spectrum taken at the lower limit of the potential window used. Other details may be found in refs 88 and 94−96.

Table 2 contains a compilation of the peak wavelengths (λ_{max}), for the various MHCF compounds considered in this review, in their oxidized and reduced states, respectively. Values of extinction coefficients are also provided, where available. The relevance of such data to the electrochromic applicability of these compounds constitutes the theme of a subsequent section. For now, the utility of UV−visible spectroelectrochemistry in studying the MHCF redox process(es) is considered. To the extent that UV−visible spectroelectrochemical data are species-specific (see above and ref 90), the trends in Table 2 do support our earlier ordering of the MHCF compounds (CuHCF < InHCF < PdHCF < CoHCF < VHCF) in terms of the redox process complexity.

Focusing now on the two more complex systems, namely, CoHCF and VHCF, Figures 12−14 contain data for CoHCF. The overlaps in the spectra for the oxidized and reduced states of CoHCF[92] manifest in terms of the bipolar character of the integral $\Delta R/R$ vs λ profiles in Figure 12 (see also Figure 3 in ref 92). The three main signatures at 380, 440, and 530 nm (Table 2) are clearly seen in the spectral evolution in Figure 12 and specially in the deconvoluted spectra in Figure 13. The evolution

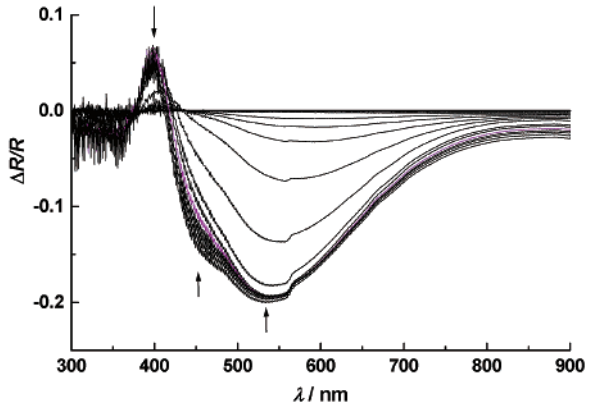

Figure 12. In situ UV−vis reflectance spectra, $\Delta R/R = [(R - R_{0.05V})/R_{0.05V}]$ for a CoHCF film in 1 M KNO_3. Spectra were collected every 0.02 V during a cyclic potential sweep at 5 mV s^{-1} in the 0.05−0.95 V range. For the sake of clarity, only a selected subset of spectra are shown and during a negative-going scan direction. Spectra were obtained at an incidence angle of 45°, with an exposure time of 0.03 s, and were averaged 20 times. All spectra are referred to the spectrum at 0.05 V. CoHCF loading: $\Gamma = 6 \times 10^{-8}$ mol cm^{-2}.

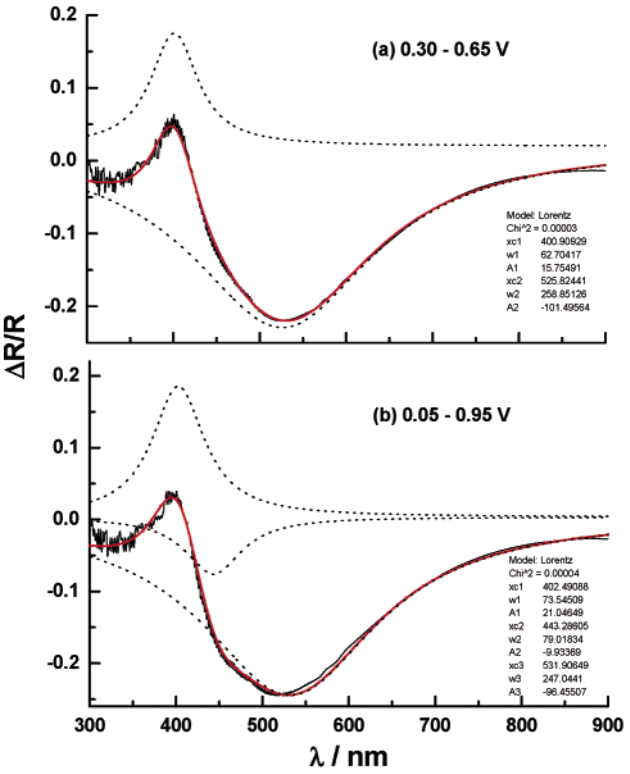

Figure 13. Deconvolution of two UV−vis difference $\Delta R/R$ spectra obtained for the potential range 0.30−0.65 V (Figure 13a) and 0.05−0.95 V (Figure 13b) for CoHCF. The characteristic parameters of the Lorentzian deconvolution are shown in each frame.

with potential of the three bands is further amplified in Figure 14. Interestingly, the two arrests in the 380-nm profile (at ∼0.50 and 0.67 V in the positive-going scan and at 0.26 and 0.40 V in the negative-going scan) suggest a 380/440- and 380/530-nm pairing of the probes for the two main redox events.

We tentatively assign the 380-nm signature to the Fe(II), Co(II) redox pairs and the 440- and 530-nm signatures to the Fe(III), Co(II) and Fe(II), Co(III) counterparts, respectively. The possibility that the 440-nm signature could have a contribution from the Fe(III), Co(III) pair (Scheme 1) is discounted by our observation that the 530-nm band intensity does not decrease while the 440-nm signature increases (Figure 14). A band at approximately this wavelength has been assigned to d−d transitions involving high-spin Co(II) sites.[97] A further discussion of the UV−visible band assignments may be found in refs 70, 97, and 98.

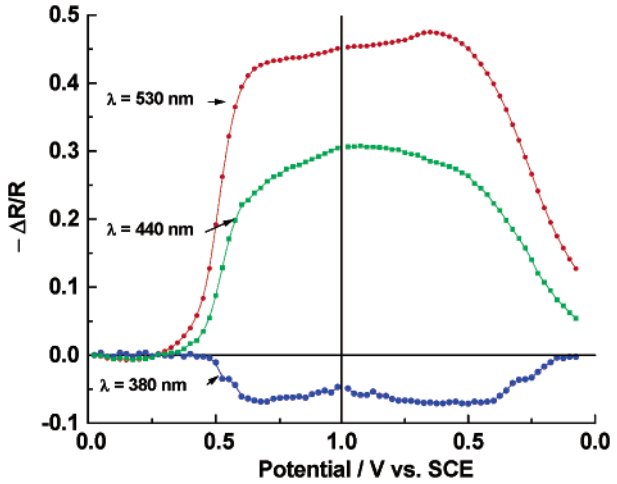

Figure 14. Evolution of the main bands peaking at 380 nm (reduced species), 440 nm (oxidized species), and 510 nm (oxidized species) for CoHCF as a function of the electrode potential. Data obtained from the spectra depicted in Figure 12.

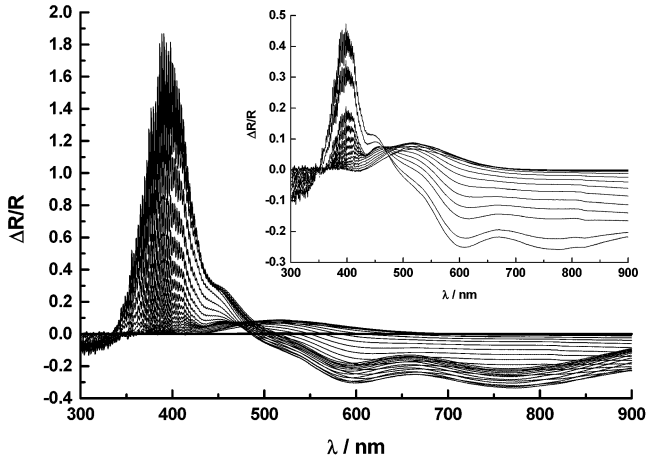

Figure 15. In situ UV−vis reflectance spectra, $\Delta R/R = [(R - R_{0.45V})/R_{0.45V}]$ for a VHCF film in 3.6 M H_2SO_4 + 0.2 M K_2SO_4. Spectra were collected every 0.025 V during a cyclic potential sweep at 5 mV s^{-1} in the 0.40−1.20 V range. For the sake of clarity, the insert contains only the spectra obtained in the 0.40−0.95 V range. All spectra are referred to the spectrum at 0.45 V. VHCF loading: 3.2×10^{-7} mol/cm^2. Other details as in Figure 12.

Turning to the VHCF system, Figures 15 and 16 contain relevant UV−visible spectroelectrochemical data. The observation of at least five spectral signatures seen in this case belies the *apparent* simplicity of the cyclic voltammogram profiles for this system that shows only two (albeit broad) sets of waves[69] (Figure 2; also see ref 14). The 600-, 780-nm set of bands may be assigned to the vanadyl (VO^{2+}) species and are implicated in the first voltammetric peak (located at more negative potentials) while the second peak is likely associated with the electrooxidation of vanadyl to vanadate (VO_2^+)

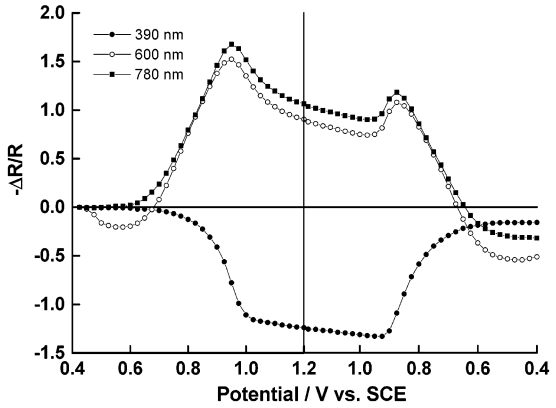

Figure 16. Evolution of the main bands peaking at 390 nm (reduced species), 600 nm (oxidized species), and 780 nm (oxidized species) as a function of electrode potential for VHCF. Data obtained from the spectra in Figure 15.

Table 3. Electrochromic Color Changes in the Various MHCF Compounds[a]

	color	
compound	reduced state	oxidized state
CuHCF	red-brown	yellow
InHCF	white	yellow
PdHCF	green	orange
CoHCF[b]	green	violet/magenta
NiHCF	grey	yellow
VHCF	yellow	blue-green

[a] Also see ref 72. [b] Color shown to depend on various factors; refer to text and refs 61 and 102.

species. Interestingly, the VO_2^+ species does not absorb in the UV−visible spectral region.[99] The evolution with potential of three selected bands for VHCF is contained in Figure 16. Relative to its counterpart in Figure 14 for CoHCF, the vanadium system appears to be considerably more complex. Further work on VHCF is needed to unravel the *chemical* details of its redox processes.

Other types of spectroelectrochemical experiments have been performed on MHCF. In situ X-ray diffraction constitutes an exceptionally powerful spectroelectrochemical probe because of the ability of X-rays to penetrate condensed phases coupled with their unparalleled structure sensitivity.[100] Such measurements have been performed on NiHCF.[101] The results from this latter study will be further discussed below within the context of ion uptake and corresponding changes in the MHCF architecture.

6. Applications of MHCF Compounds

6.1. Electrochromism. This phenomenon appears to have been given the title name in 1961 and refers to a process that involves a change in the color of a material when it either gains or loses an electron.[2] Interestingly, although the parent Prussian blue compound itself dates back to 1704, the first report on its electrochromism is relatively recent (1978).[22] Table 3 contains a summary of the color changes undergone by the other MHCF analogues (M = Cu, In, Pd, V, Co, or Ni). The Prussian blue-based electrochromic displays have been thoroughly reviewed by previous authors;[1,2] therefore, we will mainly focus on the other analogues here. It can be seen from Table 3 that all these compounds fall rather short of the electrochromic ideal figure-of-merit in terms of a color contrast from highly colored (e.g., intense blue) to completely colorless (i.e., fully light-transmissive).

Table 4. Combinations of Prussian Blue or MHCF Compounds with Other Components in Electrochromic Devices

cyanoferrate compound	complementary component	reference(s)
Prussian blue	TiO_2	48, 50
Prussian blue	$SrTiO_3$	49, 51
Prussian blue	polypyrrole	103
NiHCF	TiO_2	54, 55
CuHCF	TiO_2	55
InHCF	TiO_2	38

An interesting aspect of CoHCF films is that their color depends not only on the oxidation state of the metal centers but also on the nature of the countercations (the "A" cations in our generic structure shown in the opening paragraph of this review) and the environment. Thus, while cobalt(II) hexacyanoferrate(II) is olive-brown in the presence of hydrated K^+ or Cs^+ ions, a green color is produced upon sorption of larger cations (e.g., hydrated Na^+ or Li^+).[61,102] A reversible continuous thermochromism is observed for $K_2Co[Fe(CN)_6]\cdot nH_2O$ upon heating in the temperature range 25−85 °C.[61,70] This phenomenon is attributed to an altered environment of the Co(II) sites due to the release of bonded water molecules.[70] Whether this is a general trend for the other MHCF compounds remains to be established.

One tactic for improving the contrast in electrochromic devices is to combine two *complementary* active components.[2] Thus, either inorganic oxides (e.g., WO_3) or organic conducting polymers (e.g., polyaniline) can be combined with Prussian blue in a device.[2] Table 4 lists other combinations involving Prussian blue and MHCF analogues with complementary device components. An added advantage of using materials such as TiO_2 is that a *photoelectrochromic* mode becomes possible wherein the color change in the electrochromic material can be instigated by photoexcited charge transfer from the coupled semiconductor oxide particles.[53,54] Finally, Prussian blue itself has been mated with CuHCF in a bilayered film configuration.[104] Use of the perfluorinated ion-exchange membrane, Nafion, has been claimed to improve the stability of Prussian blue films.[105] Five-color electrochromicity has been achieved by combining Prussian blue with Nafion/methyl viologen layered films.[106] Other aspects of the electrochromism of Prussian blue and related mixed valence hexacyanometalate salts have been reviewed.[107]

6.2. Photoimage Formation. Related to the electrochromic phenomenon discussed above is the possibility of photoinduced image formation on targeted areas. This has technological relevance to displays and patterning applications. White images were successfully formed in blue films of Prussian blue-TiO_2/Nafion bilayer electrodes coated on ITO substrates.[47]

Trimetallic mixed-valence anions, $[(NC)_5Fe^{II}-CN-Pt^{IV}(NH_3)_4-NC-Fe^{II}-(CN)_5]^{4-}$ and their photoproducts, when confined in a rigid matrix, produce images on irradiation.[108,109] It has been shown that Prussian blue is formed in situ under such conditions.[108,109] The ability to generate images accrues from differences in the spectra of Prussian blue and the above anion and the resulting optical contrast between the irradiated and "dark" portions of the film. Image generation with a

scale on the order of 1 μm was demonstrated by irradiating through a mask.[108,109] This technology has been further developed by the same group using a rigid sol−gel-generated matrix incorporating the aforementioned cyanometalate complex.[110] In situ photogeneration of Prussian blue has been demonstrated earlier in an $Fe(CN)_6^{3-/4-}$-loaded chemically modified electrode containing a quaternized polyvinylpyridine layer.[111]

6.3. Ion Exchange. The possibility that the potassium countercation in MHCF compounds could be exchanged by heavier alkali metal cations was pointed out in 1965.[112] Such a strategy has practical significance for removing cesium-137 from waste streams encountered in the processing of nuclear fuels. Subsequent studies have developed this paradigm further.[113−115] The partitioning of Cs^+ and K^+ into the NiHCF film matrix was examined as a function of solution composition and the charge density on the matrix.[116] It was shown that $Cs^+ - Cs^+$ repulsive interactions limit the Cs^+ ion uptake, resulting in a stable solid composition of ~75% Cs^+ and 25% K^+ over a range of solution compositions.[116]

Other aspects of the reversible insertion electrochemistry in transition metal hexacyanometalates may be found in refs 117−121. The ion-sieving properties of self-assembled films of Prussian blue and the Co and Ni analogues were compared.[41] High separation factors (α) for Cs^+/Na^+ and K^+/Na^+ exchange were observed for Prussian blue while the α values were lower for the other two analogues.[41] The ability of ion sieving was found to increase with the membrane thickness.

Given the central importance of the details of cation partitioning into the solid phase for ion-exchange applications, it is hardly surprising that entire studies have been devoted to this topic.[101,122,123] The cubic frameworks in Figure 1 feature an open, zeolite-like structure with channel dimensions of the order of 0.32 nm. Thus, small hydrated cations such as K^+, Rb^+, Cs^+, and NH_4^+ can easily permeate the structure, while larger ions such as Na^+, Li^+, and the group II cations are blocked (see also section 4 above).

In situ XRD data acquired during ion intercalation into NiHCF showed that the lattice constant varied systematically upon cation uptake.[101] Microdomains were postulated to form when two cations having markedly different radii such as Cs^+ and K^+ were intercalated into the NiHCF network. Interestingly, the microdomains were only postulated to exist when the iron sites in the NiHCF network were in a mixed-valent (Fe^{II}, Fe^{III}) state.[101]

Assuming a 1:1 stoichiometry for the electrodeposited NiHCF analogue (Table 1), the ion-exchange process can be written as[122]

$$A_2Ni^{II}[Fe(CN)_6] \leftrightarrow A_{2-x}Ni^{II}[Fe^{II+x}(CN)_6] + xe^- + xA^- \quad (1)$$

In eq 1, x is the fraction of iron centers in the +3 oxidation state. Figure 17 contains a schematic representation of the unit cell for the oxidized and reduced forms of the NiHCF analogue. The former has four A^+ cations in the unit cell structure (see also Figure 1) while the latter accommodates eight A^+ cations in the unit cell. More generally, charge compensation dictates half as many alkali cations in the oxidized state vis-à-vis the reduced counterpart (cf. Table 1).[122]

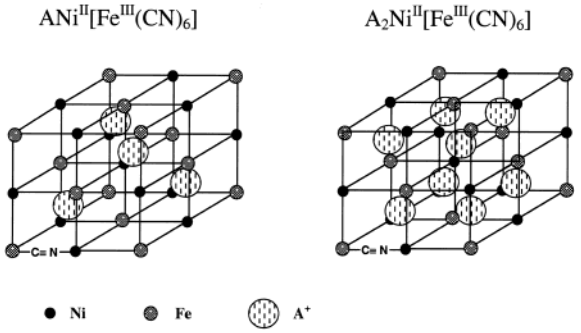

Figure 17. Unit cell representation of $ANi^{II}[Fe^{III}(CN)_6]$ and its corresponding $A_2Ni^{II}[Fe^{II}(CN)_6]$ reduced form. Four A^+ cations are in the cell interstitial sites for $ANi^{II}[Fe^{III}(CN)_6]$ and eight A^+ cations are required upon electroreduction. The cyanide groups are between Ni and Fe but have been largely omitted in this representation for the sake of clarity. See also Figure 1.

Experimental evidence from Raman spectroscopy and energy-dispersive X-ray spectroscopy (EDX) has been presented[122] in favor of a more open, nickel-rich structure than that schematized in Figure 17. The structures in Figure 17a,b are analogous to "soluble" Prussian blue, with Ni(II) and interstitial A^+ replacing the Fe(III) sites,[7] while the new data point toward a structure analogous to "insoluble" Prussian blue, with the approximate stoichiometry $K_4Ni^{II}_4[Fe(CN)_6]_3$.[122] (The quotation marks above signify that the terms "soluble" and "insoluble" refer to the ease of peptization, as also pointed out by previous authors.[2])

The "insoluble" Prussian blue analogue has a unit cell with three square planar and one octahedrally coordinated nickel atoms; all of the Fe centers are octahedrally coordinated.[123] XRD and extended X-ray absorption fine structure (EXAFS) data have been presented for cathodically deposited thin films of NiHCF in support of this structure.[123] The unit cell lattice parameter was also shown to monotonically increase from ca. 10.15 to 10.21 Å on ion exchange from 100% K^+ to 100% Cs^+.[123]

Evidence for lattice reconstruction has been presented both for NiHCF film growth on an underlying Ni substrate[124] and during redox cycling of a Prussian blue solid electrode in a K^+/Cd^{2+}-containing aqueous electrolyte.[125] Two types of ion-exchange mechanisms were postulated in the latter study based on replacement of interstitial and lattice positions, respectively.[125]

The issue of ion selectivity in the MHCF system is one that impacts both the ion-exchange and ion-sensing applications. Thus, this item is taken up in the next subsection.

6.4. Ion Sensing. Other than Prussian blue,[1] the majority of studies have focused on CuHCF and NiHCF. Early studies on CuHCF[65,66] and NiHCF[126] established trends for the cation selectivity of these host compounds. Subsequent studies[127,128] have further quantified these selectivity trends and laid the basis for both amperometric and potentiometric sensors of ammonium, alkali, and alkaline earth cations. High affinity of Tl(I) ions to CuHCF (250−100 times higher than K^+ ions) was found[129] and suggested as a basis for an electroanalytical sensor of this toxic species.

Table 5. Examples of Electrocatalysis on MHCF−Modified Electrodes

MHCF compound(s)	solution species (substrate)[a]	reference(s)
CuHCF	ascorbic acid	136
CoHCF	ascorbic acid	145
CoHCF	ascorbic acid, hydroquinone	73
CoHCF	nicotinamide adenine dinucleotide (NADH)	146
CoHCF[b]	hydrazine, thiosulfate, *p*-chlorophenol	147
CoHCF	dopamine, epinephrine, norepinephrine	148
CoHCF	NO_2^-, $S_2O_3^{2-}$, hydrazine	149
NiHCF	ascorbic acid	29, 150
NiHCF	dopamine	151
NiHCF	hydrazine	152
various analogues	SO_3^{2-}, $S_2O_3^{2-}$	60, 153
various analogues	H_2O_2	154

[a] The term "substrate" is used here in a catalysis context and refers to the solution species that are either oxidized or reduced. [b] The CoHCF compound was Ru-modified in this case.

The microstructural changes that occur in the surface derivatization layer of NiHCF[130] have been used[131] to detect $CsNO_3$ to levels as low as 10^{-8} M in the presence of 1 M $NaNO_3$. Other electroanalytically oriented studies of MHCF (mainly CuHCF) compounds may be found in refs 132−134.

Metal hexacyanoferrates have been deployed in bioanalytical applications as well. Thus, NiHCF on Ni substrates have been used for sodium and potassium assays in human whole blood serum and whole blood samples.[135] CuHCF has been utilized for analytical determination of ascorbic acid.[136] Various types of biosensors based on transition metal hexacyanoferrates and oxidase enzymes have been developed.[137−142] This topic is expected to witness rapid growth in the future, especially given the current need for new families of biosensors.

6.5. Electrocatalysis. A surface derivatization layer often imparts optimally fast electron-transfer characteristics to an underlying substrate.[62,63] This electrocatalytic phenomenon is useful from both analytical (i.e., sensor) and electrosynthetic perspectives. Examples for the good electrocatalytic activity of Prussian blue exist and have been reviewed.[1] The catalytic reduction of O_2 and CO on Prussian blue-modified electrodes has been described.[143,144]

Table 5 contains a compilation of studies on MHCF that are oriented toward electrocatalysis. While the vast majority of the earlier studies involved NiHCF, other compounds (e.g., CoHCF) are beginning to garner attention in this regard. Studies on NiHCF have also been directed toward understanding the mechanism(s) of heterogeneous electron transfer at the film/solution interface and the efficacy of electrocatalysis.[29,150−155] In this regard, the advantages with transforming an inexpensive electrode material such as Ni into a derivatized surface with electrocatalytic properties typical of expensive materials such as Pt have been pointed out.[155]

Cyclic voltammetry and hydrodynamic voltammetry constitute the most versatile probes for the efficacy of electrocatalysis.[62.63] In this manner, the locale (e.g., substrate/film, film bulk, film/solution) where rate control is exerted on the overall electrocatalysis process can be identified. This has been done for example for ascorbic acid[150] and hydrazine[152] oxidation on NiHCF-derivatized Ni substrates in aqueous media. The relationship between surface redox potential and the electrocatalysis rate constant has also been analyzed[150] within the framework of the Marcus theory.[156]

6.6. Photoelectrochemical and Photocatalytic Devices. These devices, which hinge on initial optical excitation of a semiconductor to generate electron−hole pairs, are potentially useful for photovoltaic solar energy conversion.[157,158] Given the projected importance of hydrogen in the future energy economy, such devices can also be deployed for the solar-assisted electrolysis of water.[159] Thus, simultaneous detection of H_2 and O_2 during photolysis and the photo-oxidation of water were reported in two separate studies using Prussian blue and tris(2-2′-bipyridyl) ruthenium(II) complex as cosensitizer.[160,161] A sacrificial agent is often used in such experiments.[160,162] Other authors report the co-photogeneration of H_2 and O_2 with visible light and CuHCF.[162] More work is needed to establish whether these processes are truly cyclical (except for the sacrificial agent) and to further optimize the process efficiencies.

Cadmium chalcogenide semiconductors (e.g., CdX, X = S, Se, Te), while they have yielded very high efficiencies in regenerative photoelectrochemical cells, are intrinsically unstable in aqueous media under irradiation.[157,163] On the other hand, an in situ precipitation reaction involving the photogenerated Cd^{2+} ions and solution-dosed ferrocyanide provides a protective cadmium hexacyanoferrate overlayer.[164] High light conversion efficiencies have been reported in this manner for n-CdS[165,166] and n-CdS[167,168] in aqueous ferro-/ferricyanide-containing media. Other aspects related to this interesting phenomenon, namely, the roles of Cs^+ ions in regulating photoinduced charge transfer across the n-CdX/electrolyte interface[169] and the morphology of the overlayer,[170] have been described. A thin coating of InHCF was also found to afford stabilization to n-CdSe photoanodes in aqueous media.[52]

6.7. Batteries. Given the proclivity of Prussian blue and its analogues for ion intercalation, it is not surprising that application of these materials as the active components of a battery[171] has been considered. The first study in this direction utilized the oxidation and reduction of Prussian blue respectively to Berlin green and Everitt's salt, as the two half-reactions.[172] The possibility of using other MHCF compounds was also raised in this study. A Turnbull blue (a close relative of Prussian blue, refs 1 and 2)−Nafion composite membrane was used as the active component of a rechargeable battery.[173] A combined charge storage/electrochromic display device was also constructed by the same group using Nafion and Prussian blue.[174,175] Finally, the rechargeability of battery cathodes comprising Cu/Prussian blue or Cu/Berlin green has been tested.[176]

Other MHCF compounds have been investigated as well for their applicability as battery electrodes.[177−179] Thus, a cell with NiHCF as the anode and NiHCRu (where HCRu = hexacyanoruthenate, cf., ref 1) was reported to exhibit a current efficiency of ∼100%.[178] However, a steady decrease in charge storage capacity with cycle number was noted. Solid-state secondary cells were constructed with Prussian blue as the cathode and either ZnHCF or CuHCF as the anode active material.[179] Cycle stability and charge transfer kinetics remain as two key variables that would require further optimization for Prussian blue and other MHCF com-

Table 6. Other MHCF Analogues Not Specifically Addressed in This Review[a]

compound	reference(s)
iron hexacyanoruthenate	188−190
manganese hexacyanoferrate	191
silver hexacyanoferrate	1
titanium hexacyanoferrate	192
osmium hexacyanoferrate	193
ruthenium hexacyanoferrate	194
chromium hexacyanoferrate	195

[a] See also refs 1 and 2.

pounds to effectively compete with available alternatives.

6.8. Photomagnetic and Magneto-optic Devices. The interaction of light and magnetism is a topic of much fundamental and practical interest. Molecular-based magnets offer a fertile ground for studying this interaction. Long-range ferromagnetic ordering in Prussian blue at a Curie temperature (T_c) of 5.6 K has been known for some time.[180] But only recently have a series of Prussian blue analogues begun to draw attention because of their high T_c values[181] and a value as high as 315 K has been recorded for CoHCF.[182,183] Cobalt hexacyanoferrate exhibits a photoreversible enhancement of magnetization.[9,97,184−187] Such photomagnetic effects are potentially important for applications related to optical memory, data storage, optical isolators, and the like. This topic has been thoroughly reviewed by other authors,[9,181] and the interested reader is referred to these literature sources.

6.9. Addendum. Since completion of the original draft of this review, several more papers have appeared on MHCF. Thus, a review on electrochromic materials and devices contains references on Prussian blue.[196] Prussian blue screen-printed biosensors have been described.[197] Other papers on the NiHCF system describe electrical transport as a function of temperature,[198] ac impedance,[199] and a route to diverse combinatorial libraries.[200]

7. Concluding Remarks

This review has hopefully served to underline the enormous range and scope in the chemical composition, properties, and applications of Prussian blue analogues. Six such compounds were considered in this review article. Table 6 contains a further compilation of MHCF compounds not specifically discussed above. While the earlier studies focused on Prussian blue itself, other transition metal hexacyanoferrates (and hexacyanometalates in general) are beginning to attract attention from chemists, physicists, and material scientists alike. In the crystal ball of the reviewers, this trend is expected to continue well into the future. It is our hope that this review will spur the interest of new researchers in these interesting compounds, and in a small way, will contribute to the continued vitality of this field.

Acknowledgment. This research was funded in part by a grant from the U.S. Department of Energy, Office of Basic Energy Sciences. Exchange of visits between the two participating institutions of this project was facilitated by a travel grant from the National Science Foundation (U.S.-Argentina International Programs) and CONICET, Argentina. We thank Profs. D. T. Schwartz (University of Washington) and A. B. Bocarsly (Princeton University) for preprints and discussions. Finally, the two (anonymous) reviewers are thanked for their constructive criticisms of an earlier version of the manuscript.

References

(1) Itaya, K.; Uchida, I.; Neff, V. D. *Acc. Chem. Res.* **1986**, *19*, 162; see also references therein.
(2) Monk, P. M. S.; Mortimer, R. J.; Rosseinsky, D. R. *Electrochromism: Fundamentals and Applications*; VCH: Weinheim, 1995; see also references therein.
(3) Brown, D. B. *Mixed-Valence Compounds: Theory and Applications in Chemistry, Physics, Geology and Biology*; NATO Advanced Study Institute Series; D. Reidel: Dordrecht, The Netherlands, 1980.
(4) Sharpe, A. G. *The Chemistry of Cyano Complexes of the Transition Metals*; Academic Press: New York, 1976.
(5) Chadwick, B. M.; Sharpe, A. G. *Adv. Inorg. Chem. Radiochem.* **1966**, *8*, 83.
(6) Robin, M. B.; Day, P. *Adv. Inorg. Chem. Radiochem.* **1967**, *10*, 247.
(7) Keggin, J. F.; Miles, F. D. *Nature (London)* **1936**, *137*, 577.
(8) Buser, H. J.; Schwarzenbach, D.; Petter, W.; Ludi, A. *Inorg. Chem.* **1977**, *16*, 2704.
(9) *Electrochem. Soc. Interface (Special Issue on Molecular Magnets, Fall)* **2002**, *11* (3).
(10) Ludi, A.; Gudel, H. U. In *Structure and Bonding*; Dunitz, J. D., Ed.; Springer-Verlag: Berlin, 1973; Vol. 14, pp 1−21.
(11) Herren, F.; Fischer, P.; Ludi, A.; Hälg, W. *Inorg. Chem.* **1980**, *19*, 956.
(12) West, A. R. *Basic Solid State Chemistry*; Wiley: Chichester, 1999; Chapter 1, p 25.
(13) Shaojun, D.; Fengbin, L. *J. Electroanal. Chem.* **1986**, *210*, 31.
(14) Carpenter, M. K.; Conell, R. S.; Simko, S. J. *Inorg. Chem.* **1990**, *29*, 845.
(15) Kulesza, P. J.; Malik, M. A.; Schmidt, R.; Smolinska, A.; Miecznikowski, K.; Zamponi, S.; Czerwinski, A.; Berrettoni, M.; Marassi, R. *J. Electroanal. Chem.* **2000**, *487*, 57.
(16) Kulesza, P. J.; Malik, M. A.; Skorek, J.; Smolinska, A.; Miecznikowski, K.; Zamponi, S.; Berrettoni, M.; Giorgetti, M.; Marassi, R. *J. Electroanal. Chem.* **1999**, *146*, 3757.
(17) Kulesza, P. J. *Inorg. Chem.* **1990**, *29*, 2395.
(18) Feldman, B. J.; Murray, R. W. *Inorg. Chem.* **1987**, *26*, 1702.
(19) Rosseinsky, D. R.; Tonge, J. S.; Berthold, J.; Cassidy, J. F. *J. Chem. Soc., Faraday Trans.* **1987**, *83*, 231.
(20) Xidis, A.; Neff, V. D. *J. Electrochem. Soc.* **1991**, *138*, 3637.
(21) Ayers, J. B.; Waggoner, W. H. *J. Inorg. Nucl. Chem.* **1971**, *33*, 721.
(22) Neff, V. D. *J. Electrochem. Soc.* **1978**, *125*, 886.
(23) Ellis, D.; Eckhoff, M.; Neff, V. D. *J. Phys. Chem.* **1981**, *85*, 1225.
(24) Itaya, K.; Akahoshi, H.; Toshima, S. *J. Electrochem. Soc.* **1982**, *129*, 1498.
(25) Kellawi, H.; Rosseinsky, D. R. *J. Electroanal. Chem.* **1982**, *131*, 373.
(26) Siperko L. M.; Kuwana, T. *J. Electrochem. Soc.* **1983**, *130*, 396.
(27) Bocarsly, A. B.; Sinha, S. *J. Electroanal. Chem.* **1982**, *137*, 157.
(28) Sinha, S.; Humphrey, B. D.; Fu, E.; Bocarsly, A. B. *J. Electroanal. Chem.* **1984**, *162*, 351.
(29) Sinha, S.; Humphrey, B. D.; Bocarsly, A. B. *Inorg. Chem.* **1984**, *23*, 203.
(30) Schumacher, R. *Angew. Chem., Int. Ed. Engl.* **1990**, *29*, 329.
(31) Buttry, D. A.; Ward, M. D. *Chem. Rev.* **1992**, *92*, 1355.
(32) Czirók, E.; Bácskai, J.; Kulesza, P. J.; Inzelt, G.; Wolkiewicz, A.; Mielcznikowski, K.; Malik, M. A. *J. Electroanal. Chem.* **1996**, *405*, 205.
(33) Bácskai, J.; Martinusz, K.; Czirók, E.; Inzelt, G.; Kulesza, P. J.; Malik, M. A. *J. Electroanal. Chem.* **1995**, 385, 241.
(34) Cataldi, T. R. I.; de Benedetto, G. E.; Bianchini, A. *J. Electroanal. Chem.* **1998**, *448*, 111.
(35) Lezna, R. O.; Romagnoli, R.; de Tacconi, N. R.; Rajeshwar, K. *J. Phys. Chem. B* **2002**, *106*, 3612.
(36) Cataldi, T. R. I.; Guascito, R.; Salvi, A. M. *J. Electroanal. Chem.* **1996**, *417*, 83.
(37) Reguera, E.; Bertran, J. F.; Diaz, C.; Blanco, J.; Rondon, S. *Hyperfine Interact.* **1990**, *53*, 391.
(38) de Tacconi, N. R.; Rajeshwar, K.; Lezna, R. O. *J. Electroanal. Chem.* **2001**, *500*, 270.
(39) de Tacconi, N. R.; Rajeshwar, K.; Lezna, R. O., to be published.
(40) Bharathi, S.; Nogami, M.; Ikeda, S. *Langmuir* **2001**, *17*, 7468.
(41) Pyrasch, M.; Toutianoush, A.; Jin, W.; Schnepf, J.; Tieke, B. *Chem. Mater.* **2003**, *15*, 245.
(42) Pyrasch, M.; Tieke, B. *Langmuir* **2002**, *17*, 7706.

(43) Torres, G. R.; Agricole, B.; Delhaes, P.; Mingotaud, C. *Chem Mater.* **2002**, *14*, 4012.
(44) Zhan, P.; Xue, D.; Luo, H.; Chen, X. *Nano Lett.* **2002**, *2*, 845.
(45) Rajeshwar, K.; de Tacconi, N. R.; Chenthamarakshan, C. R. *Chem. Mater.* **2001**, *13*, 2765; see also references therein.
(46) Vaucher, S.; Fielden, J.; Li, M.; Dujardin, E.; Mann, S. *Nano Lett.* **2002**, *2*, 225.
(47) Nishizawa, M.; Kuwabata, S.; Yoneyama, H. *J. Electrochem. Soc.* **1996**, *143*, 3462.
(48) De Berry, D. W.; Viehbeck, A. *J. Electrochem. Soc.* **1983**, *130*, 249.
(49) Ziegler, J. P.; Hemminger, J. C. *J. Electrochem. Soc.* **1987**, *134*, 358.
(50) Viehbeck, A.; De Berry, D. W. *J. Electrochem. Soc.* **1985**, *132*, 1369.
(51) Ziegler, J. P.; Lesniewski, E. K.; Hemminger, J. C. *J. Appl. Phys.* **1987**, *61*, 3099.
(52) Gruszecki, T.; Holmström, B. *J. Appl. Electrochem.* **1991**, *21*, 430.
(53) de Tacconi, N. R.; Carmona, J.; Rajeshwar, K. *J. Phys. Chem. B* **1997**, *101*, 10151.
(54) de Tacconi, N. R.; Carmona, J.; Balsam, W. L.; Rajeshwar, K. *Chem. Mater.* **1998**, *10*, 25.
(55) de Tacconi, N. R.; Rajeshwar, K.; Lezna, R. O. *Electrochim. Acta* **2000**, *45*, 3403.
(56) Kulesza, P. J.; Faszynska, M. *J. Electroanal. Chem.* **1988**, *252*, 461.
(57) Kulesza, P. J.; Faszynska, M. *Electrochim. Acta* **1989**, *34*, 1749.
(58) Joseph, J.; Gomathi, H.; Prabhakara Rao, G. *J. Electroanal. Chem.* **1991**, *304*, 263.
(59) Zaldivar, G. A. P.; Gushikem, Y.; Benvenutti, E. V.; de Castro, S. C.; Vasquez, A. *Electrochim. Acta* **1994**, *39*, 33.
(60) Chen, S.-M. *J. Electroanal. Chem.* **2002**, *521*, 29.
(61) Kulesza, P. J.; Malik, M. A.; Zamponi, S.; Berrettoni, M.; Marassi, R. *J. Electroanal. Chem.* **1995**, *397*, 287.
(62) Murray, R. W. In *Electroanalytical Chemistry*; Bard, A. J., Ed.; Marcel Dekker: New York, 1984; Vol. 13, p 191.
(63) Doblhofer, K.; Rajeshwar, K. In *Handbook of Conducting Polymers*; Skotheim, T. A., Elsenbaumer, R. L., Reynolds, J. R., Eds.; Marcel Dekker: New York, 1998; Chapter 20, pp 531−588.
(64) Bocarsly, A. B.; Sinha, S. *J. Electroanal. Chem.* **1982**, *140*, 167.
(65) Siperko, L. M.; Kuwana, T. *Electrochim. Acta* **1987**, *32*, 765.
(66) Engel, D.; Grabner, E. W. *Ber. Bunsen-Ges. Phys. Chem.* **1985**, *89*, 982.
(67) Gao, Z.; Wang, G.; Li, P.; Zhao, Z. *Electrochim. Acta* **1991**, *36*, 147.
(68) Malik, M. A.; Horanyi, G.; Kulesza, P. J.; Inzelt, G.; Kertesz, V.; Schmidt, R.; Czirok, E. *J. Electroanal. Chem.* **1998**, *452*, 57.
(69) de Tacconi, N. R.; Rajeshwar, K. Unpublished data, 2001−2002.
(70) Kulesza, P. J.; Malik, M. A.; Berrettoni, M.; Giorgetti, M.; Zamponi, S.; Schmidt, R.; Marassi, R. *J. Phys. Chem. B* **1998**, *102*, 1870.
(71) Jin, Z.; Dong, S. *Electrochim. Acta* **1990**, *35*, 1057.
(72) Ho, K.-C.; Chen, J.-C. *J. Electrochem. Soc.* **1998**, *145*, 2334.
(73) Jiang, M.; Zhou, M.; Zhao, Z. *Ber. Bunsen-Ges. Phys. Chem.* **1991**, *95*, 720.
(74) Lasky, S. J.; Buttry, D. A. *J. Am. Chem. Soc.* **1988**, *110*, 6258.
(75) Csahck, E.; Vieil, E.; Inzelt, G. *J. Electroanal. Chem.* **1998**, *457*, 251.
(76) Haight, S. M.; Schwartz, D. J.; Lilga, M. A. *J. Electrochem. Soc.* **1999**, *146*, 1866.
(77) Ochs, S.; Grabner, E. W.; Mohler, E. *Ber. Bunsen-Ges. Phys. Chem.* **1996**, *100*, 594.
(78) Kuwana, T.; Heineman, W. R. *Acc. Chem. Res.* **1976**, *9*, 241.
(79) Kuwana, T.; Winograd, N. In *Electroanalytical Chemistry*; Bard, A. J., Ed.; Marcel Dekker: New York, 1974; Vol. 7, Chapter 1.
(80) Heineman, W. R.; Hawkridge, F. M.; Blount, H. N. In *Electroanalytical Chemistry*; Bard, A. J., Ed.; Marcel Dekker: New York, 1984; Vol. 13, Chapter 1.
(81) Heineman, W. R. *J. Chem. Educ.* **1983**, *60*, 305; see also references therein.
(82) Gale, R. J., Ed.; *Spectroelectrochemistry: Theory and Practice*; Plenum: New York, 1988.
(83) Rajeshwar, K.; Lezna, R. O.; de Tacconi, N. R. *Anal. Chem.* **1992**, *64*, 429A.
(84) Ghosh, S. N. *J. Inorg. Nucl. Chem.* **1974**, *36*, 2465.
(85) Hester, R. E.; Nour, E. M. *J. Chem. Soc., Dalton Trans.* **1981**, 938.
(86) Nakamoto, K. *Infrared and Raman Spectra of Inorganic and Coordination Compounds*, 5th ed.; John Wiley: New York, 1997.
(87) Steen, W. A.; Jeerage, K. M.; Schuartz, D. T. *Appl. Spectrosc.* **2002**, *56*, 1021.
(88) Lezna, R. O.; Romagnoli, R.; de Tacconi, N. R.; Rajeshwar, K. *J. Electroanal. Chem*, **2003**, *544*, 101.
(89) Arancibia, V.; Beden, B.; Leger, J.-M.; de Tacconi, N. R.; Lezna, R. O. In *Molecular Functions of Electroactive Thin Films*; Oyama, N., Birss, V., Eds.; The Electrochemical Society: Pennington, NJ; 1998, Proceedings Volume 98-26, pp 114−119.
(90) Humphrey, B. D.; Sinha, S.; Bocarsly, A. B. *J. Phys. Chem.* **1984**, *88*, 736.
(91) Son, Y.; Rajeshwar, K. *J. Chem. Soc., Faraday Trans.* **1992**, *88*, 605.
(92) Kulesza, P. J.; Zamponi, S.; Malik M. A.; Berrettoni, M.; Wolkiewicz, A., Marassi, R. *Electrochim. Acta* **1998**, *43*, 919.
(93) De Angelis, T. P.; Heineman, W. R. *J. Chem. Educ.* **1976**, *53*, 594.
(94) Lezna, R. O.; de Tacconi, N. R.; Rapallini, J. A.; Arvia, A. J. *An. Asoc. Quim. Argent.* **1988**, *76*, 25.
(95) Juanto, S.; Lezna, R. O. Arvia, A. J. *Electrochim. Acta* **1994**, *39*, 81.
(96) Lezna, R. O.; Juanto, S.; Zagal, J. H. *J. Electroanal. Chem.* **1995**, *389*, 197.
(97) Sato, O.; Einaga, Y.; Fujishima, A.; Hashimoto, K. *Inorg. Chem.* **1999**, *38*, 4405.
(98) Bleuzen, A.; Lomenech, C.; Escax, V.; Villain, F.; Varret, F.; Cartier dit Moulin, Ch.; Verdaguer, M. *J. Am. Chem. Soc.* **2000**, *122*, 6648.
(99) Parish, R. V. *The Metallic Elements*; Longman: London, 1977; p 76.
(100) Abruña, H. D. Ed.; *Electrochemical Interfaces: Modern Techniques for In Situ Interface Characterization*; VCH: New York, 1991.
(101) Kelly, M. T.; Arbuckle-Keil, G. A.; Johnson, L. A.; Su, E. Y.; Amos, L. J.; Chun, J. K. M.; Bocarsly, A. B. *J. Electroanal. Chem.* **2001**, *500*, 311.
(102) Kulesza, P. J.; Malik, M. A.; Miecznikowski, K.; Wolkiewicz, A.; Zamponi, S.; Berrettoni, M.; Marassi, R. *J. Electrochem. Soc.* **1996**, *143*, L10.
(103) Leventis, N.; Chung, Y. C. *Chem. Mater.* **1992**, *4*, 1415.
(104) Siperko, L. M.; Kuwana, T. *J. Electrochem. Soc.* **1986**, *133*, 2439.
(105) Garcia-Jareño, J. J.; Navarro-Laboulais, J.; Vicente, F. *Electrochim. Acta* **1996**, *41*, 2675.
(106) Mortimer, R. J. *J. Electrochem. Soc.* **1991**, *138*, 633.
(107) Mortimer, R. J. *Chem. Soc. Rev.* **1993**, *26*, 147.
(108) Wu, Y.; Pfenning, B. W.; Bocarsly, A. B. *Inorg. Chem.* **1995**, *34*, 4262.
(109) Bocarsly, A. B.; Chang, C. C.; Wu, Y.; Vicenzi, E. P. *J. Chem. Educ.* **1997**, *74*, 663.
(110) Watson, D. F.; Willson, J. L.; Bocarsly, A. B. *Inorg. Chem.* **2002**, *41*, 2408.
(111) Basak, S.; Rajeshwar, K.; Kaneko, M. *J. Electroanal. Chem.* **1990**, *295*, 403.
(112) Prout, W. E.; Russell, E. R.; Groh, H. J. *J. Inorg. Nucl. Chem.* **1965**, *27*, 473.
(113) Lilga, M. A.; Orth, R. J.; Sukamto, J. P. H.; Haight, S. M.; Schwartz, D. T. *Sep. Purif. Technol.* **1997**, *11*, 147.
(114) Rassat, S. D.; Sukamto, J. H.; Orth, R. J.; Lilga, M. A.; Hallen, R. T. *Sep. Purif. Technol.* **1999**, *15*, 207.
(115) Jeerage, K. M.; Schwartz, D. T. *Sep. Purif. Technol.* **2000**, *35*, 2375.
(116) Jeerage, K. M.; Steen, W. A.; Schwartz, D. T. *Langmuir* **2002**, *18*, 3620.
(117) Ayrault, S.; Loos-Neskovic, C.; Fedoroff, M.; Garnier, E.; Jones, D. J. *Talanta* **1995**, *42*, 1581.
(118) Scholz, F.; Dostal, A. *Angew. Chem., Int. Ed. Engl.* **1995**, *34*, 2685.
(119) Dostal, A.; Hermes, M.; Scholz, F. *J. Electroanal. Chem.* **1996**, *415*, 133.
(120) Widmann, A.; Kahlert, H.; Petrovic-Prelevic, I.; Wulff, H.; Yakhmi, J. V.; Bagkar, N. Scholz, F. *Inorg. Chem.* **2002**, *41*, 5706.
(121) Liu, C.; Wang, Y.; Zhu, G.; Dong, S. *Electrochim. Acta* **1997**, *42*, 1795.
(122) Jeerage, K. M.; Steen, W. A.; Schwartz, D. T. *Chem. Mater.* **2002**, *14*, 530.
(123) Steen, W. A.; Han, S.-W.; Yu, Q.; Gordon, R. A.; Cross, J. O.; Stern, E. A.; Seidler, G. T.; Jeerage, K. M.; Schwartz, D. T. *Langmuir* **2002**, *18*, 7714.
(124) Amos, L. J.; Schmidt, M. H.; Sinha, S.; Bocarsly, A. B. *Langmuir* **1986**, *2*, 559.
(125) Dostal, A.; Meyer, B.; Scholz, F.; Schröder, U.; Bond, A. M.; Marken, F.; Shaw, S. J. *J. Phys. Chem.* **1995**, *99*, 2096.
(126) Schneemeyer, L. F.; Spengler, S. E.; Murphy, D. W. *Inorg. Chem.* **1985**, *24*, 3044.
(127) Thomsen, K. N.; Baldwin, R. P. *Anal. Chem.* **1989**, *61*, 2594.
(128) Tani, Y.; Eun, H.; Umezawa, Y. *Electrochim. Acta* **1998**, *43*, 3431.
(129) Zadronecki, M.; Linek, I. A.; Stroka, J.; Wrona, P. K.; Galus, Z. *J. Electrochem. Soc.* **2001**, *148*, E 348.
(130) Sinha, S.; Amos, L. J.; Schmidt, M. H.; Bocarsly, A. B. *J. Electroanal. Chem.* **1986**, *210*, 323.
(131) Amos, L. J.; Duggal, A.; Mirsky, E. J.; Ragonesi, P.; Bocarsly, A. B.; Fitzgerald-Bocarsly, P. A. *Anal. Chem.* **1988**, *60*, 245.
(132) Zaldivar, G. A. P.; Gushikem, Y.; Kubato, L. *J. Electroanal. Chem.* **1991**, *318*, 247.
(133) Malik, M. A.; Kulesza, P. J. *Electroanalysis* **1996**, *8*, 113.
(134) Xu, J.-J.; Fang, H.-Q.; Chen, H.-Y. *J. Electroanal. Chem.* **1997**, *426*, 139.

(135) Coon, D. R.; Amos, L. J.; Bocarsly, A. B.; Fitzgerald-Bocarsly, P. A. *Anal. Chem.* **1998**, *70*, 3137.
(136) Shankaran, D. R.; Narayanan, S. S. *Fresnius J. Anal. Chem.* **1999**, *364*, 686.
(137) Karyakin, A. A.; Gitelmacher, O. V.; Karyakina, E. E. *Anal. Lett.* **1994**, *27*, 2861.
(138) Karyakin, A. A.; Gitelmacher, O. V.; Karyakina, E. E. *Anal. Chem.* **1995**, *67*, 2419.
(139) Karyakin, A. A.; Karyakina, E. E.; Gorton, L. *Talanta* **1996**, *43*, 1597.
(140) Karyakin, A. A.; Karyakina, E. E.; Gorton, L. *Electrochem. Commun.* **1999**, *1*, 78.
(141) Karyakin, A. A.; Karyakina, E. E.; Gorton, L. *J. Electroanal. Chem.* **1998**, *456*, 97.
(142) Karyakin, A. A.; Karyakina, E. E.; Gorton, L. *Anal. Chem.* **2000**, *72*, 1720.
(143) Itaya, K.; Shoji, N.; Uchida, I. *J. Am. Chem. Soc.* **1984**, *106*, 3423.
(144) Ogura, K.; Kaneko, M. *J. Mol. Catal.* **1985**, *31*, 49.
(145) Cai, C.-X.; Xue, K.-H.; Xu, S.-M. *J. Electroanal. Chem.* **2000**, *486*, 111.
(146) Cai, C.-X.; Ju, H.-X.; Chen, H.-Y. *J. Electroanal. Chem.* **1995**, *397*, 185.
(147) Cataldi, T. R. I.; De Benedetto, G.; Bianchini, A. *J. Electroanal. Chem.* **1999**, *471*, 42.
(148) Chen, S.-M.; Peng, K.-T. *J. Electroanal. Chem.* **2003**, *547*, 179.
(149) Chen, S.-M. *Electrochim. Acta* **1998**, *43*, 3359.
(150) Humphrey, B. D.; Sinha, S.; Bocarsly, A. B. *J. Phys. Chem.* **1987**, *91*, 586.
(151) Zhou, D.-M.; Ju, H.-X.; Chen, H.-Y. *J. Electroanal. Chem.* **1996**, *408*, 219.
(152) Lin, C.; Bocarsly, A. B. *J. Electroanal. Chem.* **1991**, *300*, 325.
(153) Chen, S.-M. *J. Electroanal. Chem.* **1996**, *417*, 145.
(154) Garjonyte, R.; Malinauskas, A. *Sensors Actuators B* **1998**, *46*, 236.
(155) Bocarsly, A. B.; Galvin, S. A.; Sinha, S. *J. Electrochem. Soc.* **1983**, *130*, 1319.
(156) Marcus, R. A. *J. Electroanal. Chem.* **1997**, *438*, 251; see also references therein.
(157) Rajeshwar, K. In *Encyclopedia of Electrochemistry*; Licht, S., Ed.; Wiley-VCH: Weinheim, 2001; Chapter 1, pp 3−53.
(158) Rajeshwar, K. In *Electron Transfer in Chemistry*; Balzani, V., Ed.; Wiley-VCH: Weinheim, 2001.
(159) Archer, M. D.; Nozik, A. J. Eds.; *Photochemical and Photoelectrochemical Approaches to Solar Energy Conversion*; Imperial College Press: London, in press.
(160) Christensen, P. A.; Harriman, A.; Neta, P.; Richoux, M. C. *J. Chem. Soc., Faraday Trans.* **1985**, *81*, 2461.
(161) Kaneko, M.; Takabayashi, N.; Yamauchi, Y.; Yamada, A. *Bull. Chem. Soc. Jpn.* **1984**, *57*, 156.
(162) Tennakone, K.; Wickramanayake, S.; Fernando, N. *Sol. Energy Mater.* **1987**, *16*, 467.
(163) Rajeshwar, K. *J. Appl. Electrochem.* **1985**, *15*, 1; see also references therein.
(164) Bocarsly, A. B. *Chem., Ind.* **1992**, 2 Nov, 813; see also references therein.
(165) Rubin, H.-D.; Humphrey, B. D.; Bocarsly, A. B. *Nature* **1984**, *308*, 339.
(166) Rubin, H.-D.; Arent, D. J.; Humphrey, B. D.; Bocarsly, A. B. *J. Electrochem. Soc.* **1987**, *134*, 93.
(167) Rubin, H.-D.; Arent, D. J.; Bocarsly, A. B. *J. Electrochem. Soc.* **1985**, *132*, 523.
(168) Arent, D. J.; Rubin, H.-D.; Chen, Y.; Bocarsly, A. B. *J. Electrochem. Soc.* **1992**, *139*, 2705.
(169) Arent, D. J.; Hidalgo-Luangdilok, C.; Chun, J. K. M.; Bocarsly, A. B.; Woods, R. E. *J. Electroanal. Chem.* **1992**, *328*, 295.
(170) de Tacconi, N. R.; Myung, N.; Rajeshwar, K. *J. Phys. Chem.* **1995**, *99*, 6103.
(171) For example: Owen, J. R. *Chem. Soc. Rev.* **1997**, *26*, 259.
(172) Neff, V. D. *J. Electrochem. Soc.* **1985**, *132*, 1382.
(173) Honda, K.; Ochiai, J.; Hayashi, H. *J. Chem. Soc., Chem. Commun.* **1986**, 168.
(174) Honda, K.; Kuwano, A. *J. Electrochem. Soc.* **1986**, *133*, 853.
(175) Honda, K.; Hayashi, H. *J. Electrochem. Soc.* **1987**, *134*, 1330.
(176) Kuwabara, K.; Nunome, J.; Sugiyama, K. *Solid State Ionics* **1991**, *58*, 303.
(177) Grabner, E. W.; Kalwellis-Mohn, S. *J. Appl. Electrochem.* **1987**, *17*, 653.
(178) Kalwellis-Mohn, S.; Grabner, E. W. *Electrochim. Acta* **1989**, *34*, 1265.
(179) Jayalakshmi, M.; Scholz, F. *J. Power Sources* **2000**, *91*, 217.
(180) Hoden, A. N.; Matthias, B. T.; Anderson, P. W.; Luis, H. W. *Phys. Rev.* **1956**, *102*, 1463.
(181) Ohkoshi, S−i.; Hashimoto, K. *J. Photochem. Photobiol. C: Photochem Rev.* **2001**, *2*, 71.
(182) Ferlay, S.; Mallak, T.; Ouahès, R.; Vellet, P.; Verdaguer, M. *Nature* **1995**, *378*, 701.
(183) Dujardin, E.; Ferlay, S.; Phan, X.; Desplanches, C.; Cartier dit Moulin, C.; Sainctavit, P.; Baudelet, F.; Dartyge, E.; Veillet, P.; Verdaguer, M. *J. Am. Chem. Soc.* **1998**, *120*, 11347.
(184) Sato, O.; Iyoda, T.; Fujishima, K.; Hashimoto, K. *Science* **1996**, *272*, 704.
(185) Verdaguer, M. *Science* **1996**, *272*, 698.
(186) Sato, O.; Einaga, Y.; Iyoda, T.; Fujishima, A.; Hashimoto, K. *J. Electrochem. Soc.* **1997**, *144*, 11.
(187) Champion, G.; Cartier dit Moulin, C.; Villain, F.; Bleuzen, A.; Baudelet, F.; Dartyge, E.; Verdaguer, M. *J. Am. Chem. Soc.* **2001**, *123*, 12544; see also references therein.
(188) Rajan, K. P.; Neff, V. D. *J. Phys. Chem.* **1982**, *86*, 4361.
(189) Itaya, K.; Ataka, T.; Toshima, S. *J. Am. Chem. Soc.* **1982**, *104*, 3751.
(190) Cox, J. A.; Kulesza, P. J. *Anal. Chem.* **1984**, *56*, 1021.
(191) Bharathi, S.; Joseph, J.; Jeyakumar, D.; Prabhakara Rao, G. *J. Electroanal. Chem.* **1991**, *319*, 341.
(192) Jiang, M.; Zhou, X. Y.; Zhao, Z. F. *J. Electroanal. Chem.* **1990**, *292*, 289.
(193) Cox, J. A.; Das, B. K. *J. Electroanal. Chem.* **1987**, *233*, 87.
(194) Kulesza, P. J. *J. Electroanal. Chem.* **1987**, *220*, 295.
(195) Eftekhari, A. *J. Power Sources* **2003**, *117*, 249.
(196) Somani, P. R.; Radhakrishnan, S. *Mater. Chem. Phys.* **2002**, *77*, 117.
(197) Ricci, F.; Amine, A.; Palleschi, G.; Mosconi, D. *Biosens. Bioelectron.* **2003**, *18*, 165.
(198) El-Sayed, B. A.; Shabana, A. A.; Abo-Aly, M. M.; Sallam, M. M. *J. Mater. Sci.: Mater. Electron.* **2003**, *14*, 27.
(199) Retter, U.; Widmann, A.; Siegler, K.; Kahlert, H. *J. Electroanal. Chem.* **2003**, *546*, 87.
(200) Steen, W. A.; Schwartz, D. T. *Chem. Mater.* **2003**, *15*, 2449.

CM0341540